BNL--51940

DE86 005300

BNL 51940
UC-93
(Energy Conversion - TIC-4500)

PHOTOVOLTAIC-POWERED SOLID POLYMER ELECTROLYTE (SPE) ELECTROLYZER SYSTEM EVALUATION

FINAL REPORT

Philip D. Metz and Michael Piraino

July 1985

ENERGY APPLICATIONS AND ANALYSIS DIVISION
DEPARTMENT OF APPLIED SCIENCE
BROOKHAVEN NATIONAL LABORATORY
ASSOCIATED UNIVERSITIES, INC.

UNDER CONTRACT NO. DE-AC02-76CH00016 WITH THE
UNITED STATES DEPARTMENT OF ENERGY

Printed in the United States of America
Available from
National Technical Information Service
U.S. Department of Commerce
5285 Port Royal Road
Springfield, VA 22161

NTIS price codes:
Printed Copy: A04; Microfiche Copy: A01

TABLE OF CONTENTS

LIST OF TABLES

LIST OF FIGURES

EXECUTIVE SUMMARY

This report presents the final results of the evaluation of a photovoltaic-powered solid polymer electrolyte (SPE) electrolyzer system at the Brookhaven National Laboratory (BNL) Hydrogen Technology Evaluation Center (HTEC). This represents the completion of the first major evaluation effort at the HTEC facility. The results of electrolyzer system operation are examined to measure component performance, validate a computer simulation model of the system, and examine the economics of such systems.

HTEC Facility

The BNL HTEC facility has been built to test and analyze more efficient and less expensive methods of producing, storing, transporting, and using hydrogen as an energy source. The purpose of the Center is to:

- Evaluate advanced hydrogen energy systems.
- Promote hydrogen technology transfer to the commercial sector.
- Provide a hands-on learning tool for hydrogen energy systems.
- Promote cooperative R&D with the public and private sectors in the U.S. including DOE, DOD, NASA, and private industry.
- Foster international cooperation in hydrogen technology within the framework of the International Energy Agency (IEA).

To accomplish these goals, the Center has been designated a User's Facility, which makes it available to users from industry, universities, and other government laboratories.

Electrolyzer System Test Results

The PV-powered electrolyzer system has been operated between December 1983 and July 1985 in three different modes:

- Grid-powered electrolyzer operation
- 300% Boosted PV-powered operation
- Complementary PV plus grid-powered operation

The system was installed in December 1983. Initial operation was far from smooth, with frequent automatic shutdowns due to malfunctions in sensors, controls, the data acquisition system, and the process water system. In June 1984, the SPE module was found to leaking hydrogen into the oxygen system due to contamination during assembly.

A rebuilt module was installed in December 1984. The average number of shutdowns/day was gradually reduced from 0.9 for the first module to 0.2 with the second.

It is clear that cleanliness is a paramount concern in the SPE system. This characteristic adds complexity and reliability problems, and must be dealt with.

B199
SPE(ES)1

The PV array operated very reliably at an efficiency of approximately 8%. The array output voltage, controlled by a DC-DC converter, averaged 29-30 VDC. The DC-DC converter efficiency was found to average 75%, much lower than the 94% shown by our computer simulation model to be necessary to compete with an optimal directly coupled system.

SPE electrolyzer performance results were obtained for temperatures between 50-75°C. With the replacement module, voltage efficiency was found to range from 97% at 82 A/ft^2 (53°C) to 83% at 1003 A/ft^2 (75°C). No significant performance difference was found between grid-powered and solar-powered electrolyzer operation. Further, observed efficiencies were within 4% of those predicted by the simulation model, which is based on manufacturer's data, thus validating this model.

Transient Simulation Results

A transient simulation model of PV-powered electrolyzer systems was developed, based on the transient simulation computer program TRNSYS. Innovative features of the modeling include the use of real weather data and detailed hourly modeling of the PV array thermal characteristics and control strategies. A wide range of system voltage and power ratings were examined in both the directly-coupled and maximum power tracking (MPT) modes.

For directly-coupled systems, the model shows that the optimal PV array voltage is very close to the nominal maximum electrolyzer voltage for a wide range of PV array sizes. An optimal directly-coupled system performs 94% as well as a perfect MPT system. Thus, the value of power trackers appears dubious for these systems.

Technoeconomic Analysis

Based on the system simulation model, an economic model which computes the cost of producing hydrogen electrolytically was developed. The economic model is quite simple (e.g., does not consider depreciation, income tax consequences or inflation) so tht absolute comparisons between the hydrogen costs generated and real-world market prices should be viewed cautiously. However, the simplicity of the model makes relative comparisons between different operating modes and sensitivity analyses of capital costs, electricity costs, etc. quite transparent. Three modes of operation have been considered:

- Grid-Powered Operation
- Stand-Alone PV-Powered Operation
- PV Supplemented by 8-Hour/day Off-Peak Grid Electricity

Of the three options studied, the grid-powered system produced the least costly hydrogen--usually by a wide margin, followed by the combined system, and then by the stand-alone PV system. For the two PV cases, the economic model developed can be used to determine the optimal relative PV array size.

B199
SPE(ES)2

Economically, a grid-powered electrolyzer can compete with natural gas reformer-derived hydrogen if electrolyzer capital cost is low. A stand-alone PV-powered system cannot, due to the high cost of PV-derived electricity and poor electrolyzer capital utilization. A combined PV-grid system is marginal, and can provide a hedge against future electricity price increases.

B199
SPE (ES)3

1.0 INTRODUCTION

1.1 Scope of This Report

This report presents the final results of the evaluation of a photovoltaic-powered solid polymer electrolyte (SPE) electrolyzer system at the Brookhaven National Laboratory (BNL) Hydrogen Technology Evaluation Center (HTEC). Section 1 introduces the HTEC facility and the SPE electrolyzer system. In Section 2, electrolyzer system test results are presented. Section 3 is a technoeconomic analysis of hydrogen production via PV-powered electrolysis and other options. The use of grid versus photovoltaic electricity is evaluated parametrically. Appendix I presents PV-electrolyzer system transient computer simulation results. Appendix II describes the economic model on which the technoeconomic analysis in Section 3 is based. Appendix III presents Fitting Equations and Coefficients of some of the test results.

1.2 Hydrogen Technology Evaluation Center at Brookhaven National Laboratory

Purpose

The Hydrogen Technology Evaluation Center (HTEC) at Brookhaven National Laboratory is a facility built to test and analyze more efficient and less expensive methods of producing, storing, transporting, and using hydrogen as an energy source. The purpose of the Center is to:

- Evaluate advanced hydrogen energy systems.
- Promote hydrogen technology transfer to the commercial sector.
- Provide a hands-on learning tool for hydrogen energy systems.
- Promote cooperative R&D with the public and private sectors in the U.S. including DOE, DOD, NASA, and private industry.
- Foster international cooperation in hydrogen technology within the framework of the International Energy Agency (IEA).

To accomplish these goals, the Center has been designated a User's Facility, which makes it available to users from industry, universities, and other government laboratories. Arrangements are made on an individual basis.

Activities

Activities at the Hydrogen Technology Evaluation Center fall into three main categories:

- Characterize inexhaustible resource energy conversion options.
- Integrate advanced concepts for hydrogen production, storage, transport, and end use.
- Perform energy system simulation and economic analysis.

Evaluation of the SPE electrolyzer system was the first major investigation at the HTEC facility. Another major effort, recently completed, was the evaluation of a heat-actuated metal-hydride hydrogen compressor. Future plans

call for the evaluation of novel hydrogen liquefaction systems based on magnetic cooling or thermally-actuated metal hydride compressors.

Technical Approach

System evaluations are carried out at HTEC via a coordinated program with three key elements:

- Hardware characterization
- Computer simulation
- Economic analysis

Hardware testing on this pilot scale measures component performance and system behavior, while validating analytical component models and computer simulation results. Computer simulations answer questions about long-term system behavior and control strategy which would take years to answer experimentally. The simulations form the basis for economic analyses of hydrogen energy systems.

Facility Design

Figure 1.1 is a photograph of the HTEC facility. Visible in front of the building is the 5 kW photovoltaic array which partially powers the SPE electrolyzer.

Figure 1.2 is a cutaway view of the HTEC building. Room 1 is a clean room housing the data acquisition/control subsystem, including a computer used for electrolyzer system modeling. Room 2 is a small utility room containing the power conditioning equipment for the electrolyzer. The SPE electrolyzer itself, is located in room 3, along with its associated water treatment system, hydrogen dryer, and safety devices. Room 4 contains a test system for characterizing heat-actuated metal-hydride hydrogen compressors. A walkway is provided for visitors to view the facility.

1.3 Solid Polymer Electrolyte System

Energy Conversion Subsystem

Figure 1.3 is a schematic of the SPE electrolyzer system as tested at HTEC. Electricity is provided to the electrolyzer from two sources: the utility grid and a 5-kW photovoltaic (PV) array. The flat-plate PV array, manufactured and installed by Solarex Corporation, and shown in Figure 1.1, provides a peak power output of about 5 kW at a solar insolation level of 1 kW/m^2 normal to the array. The optimal array operating voltage is approximately 32 V.

Solar electricity is supplied to a computer-controlled DC-DC converter which, acting as a sort of "DC transformer," maximizes the power output from the PV array. A computer-controlled power supply provides rectified grid power. These two devices, acting in parallel, power the SPE electrolyzer as shown in Figure 1.3.

The General Electric SPE electrolyzer module is pictured in Figure 1.4. The 1000 cm^2 (1 ft^2), 8-cell module operates at current densities up to about 1000 A/ft^2 at efficiencies of roughly 80-90%. The module consumes about 15 kW of electricity when operating at its maximum current of 1000 Amperes. Detailed performance results are presented in Section 2.

The electrolyzer console is also shown in Figure 1.4, above and to the right of the module. The console contains control electronics, process-water, and gas-handling ancillaries. To date, all hydrogen produced by the SPE electrolyzer system has been dried and then vented.

Data Acquisition/Control Subsystem

The data acquisition/control subsystem monitors and controls the energy conversion hardware described above. Analog sensors which monitor temperatures, voltages, currents, flow rates, etc. are scanned approximately once every three seconds by a Fluke Model 2400-A "smart" datalogger. This device then digitizes and converts these data inputs to engineering units. The datalogger, under direction of a Fluke 1720-A Microcomputer, transmits control signals and alarms to the electrolyzer, the DC-DC converter, and the power supply. Data, after being averaged and stored temporarily in the 1720-A computer, is downloaded hourly to the data acquisition/analysis computer, an IBM 9000, for permanent storage and analysis.

Figure 1.1 HTEC facility showing 5-kW photovoltaic array.

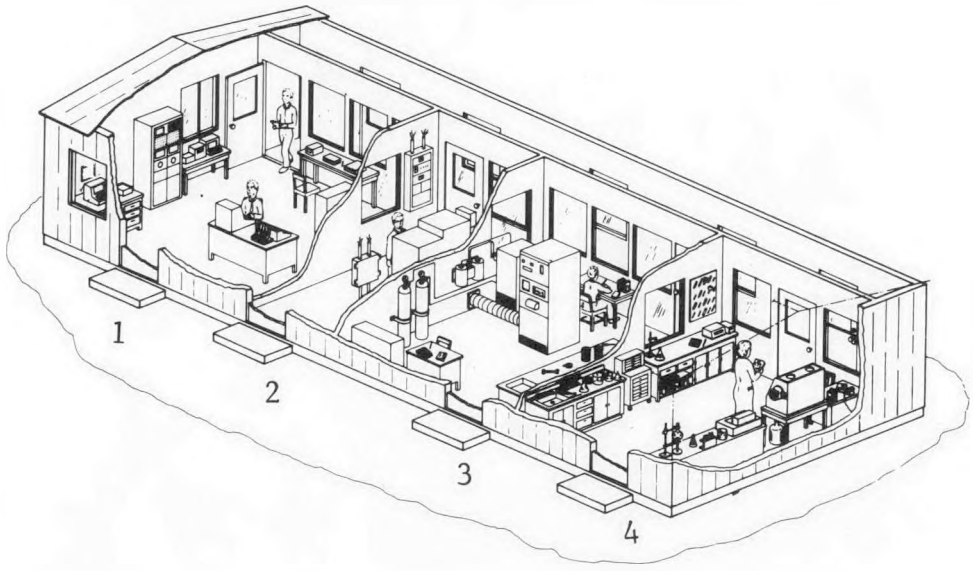

Figure 1.2 Cutaway view of HTEC building.

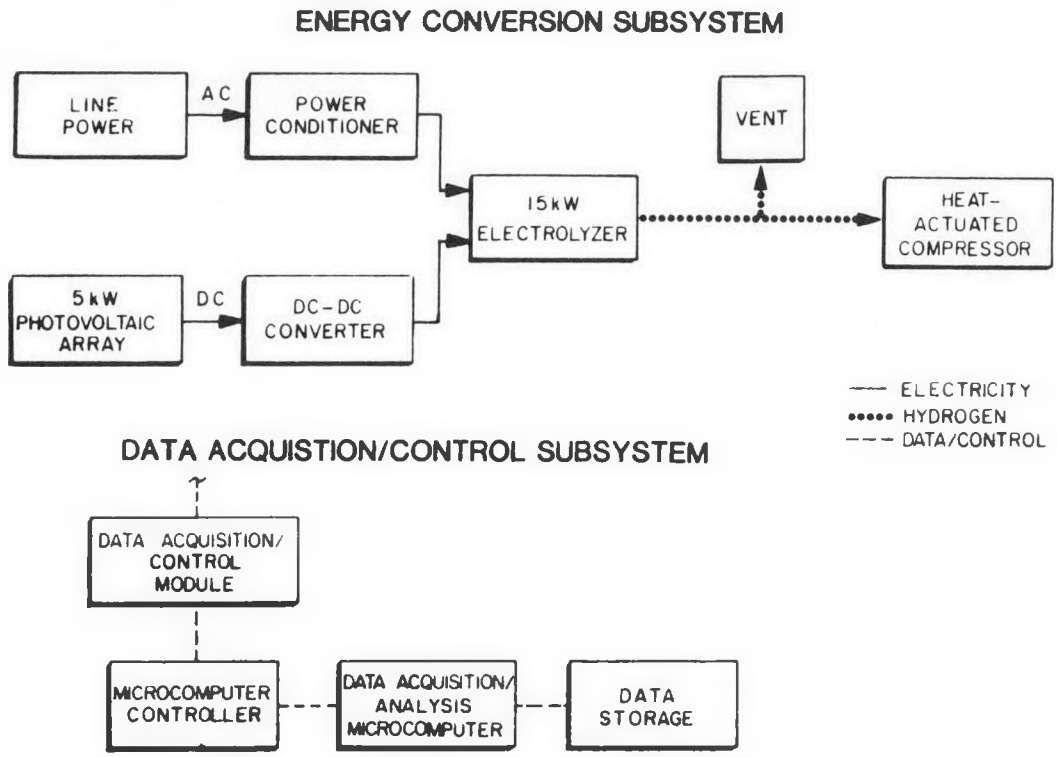

Figure 1.3 Schematic of SPE electrolyzer system.

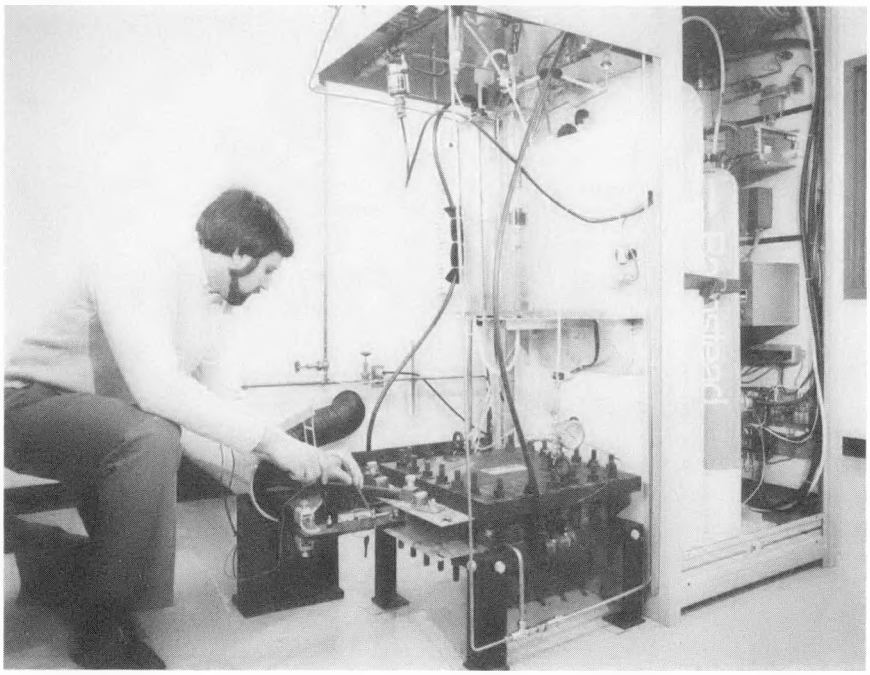

Figure 1.4 SPE electrolyzer module (bottom center) and console (cover removed).

2.0 ELECTROLYZER SYSTEM TEST RESULTS

2.1 Operating Modes

The PV-powered electrolyzer system described in Section 1 has been operated between December 1983 and July 1985 in three different modes:

- Grid-powered electrolyzer operation.
- 300% boosted PV-powered operation.
- Complementary PV-plus grid-powered operation.

Grid-powered electrolyzer operating tests were conducted periodically at several constant power levels to provide baseline performance data. Baseline test results are presented in Section 2.3, and compared to PV-powered test results and simulation results in Section 2.5.

In the 300% boosted PV-powered operating mode, the PV-derived output of the DC-DC converter (see system schematic Figure 1.3) is augmented by 300% using the computer-controlled power supply. The power supply output is updated approximately every 3 seconds by the data acquisition/control subsystem so that the 5kW PV array output is tracked quite accurately. The result is that the SPE electrolyzer "sees" a power source which behaves like a 15kW PV array.

In the complementary PV-plus grid-powered operating mode, the SPE electrolyzer is operated at a preselected constant power level. The PV array, through the DC-DC converter, provides as much energy as possible, with the computer-controlled power supply making up the balance. All solar-powered operating results are presented in Section 2.4.

2.2 Chronology of Operation

This section presents a chronology of electrolyzer system operation between December 1983 and July 1985, followed by a brief discussion.

December 1983: The electrolyzer system, including the data acquisition/control subsystem was installed by GE engineers and BNL technicians (the PV array was installed by Solarex Corporation in Fall 1983).

January 1984: System shakedown operation began. Sensors were tested and minor repairs performed. Some limited system operation was possible.

February 1984: Full operation was attempted. However, the system was unable to operate properly in any solar-powered mode because the maximum power tracking software controlled the DC-DC converter incorrectly. New software was developed to solve this problem, but system operation was plagued by gas sensor and process water system malfunctions which shut down the electrolyzer.

B199
SPE(2)1

March-June 1984: Between March 8 and June 21 the system was operated in all 3 modes described above as follows:

Type of Operation: Module power weekdays, ancillaries at night and weekends (Beginning April 2).

Total Number of Weekdays: 76

Weekdays with No Daytime Operation: 32

Cause	Days
GE repairs	2
Datalogger repairs	6
Process water pump repairs	11
Gas sensors	6
H_2 plumbing revisions	3
DC-DC converter repairs	2
Sensor calibration	1
N_2 regulator used for test	1
TOTAL	32

Weekdays with Daytime Operation: 44

Average Hours Per Day: 6.2

Total Number of System Shutdowns: 40

Average Shutdowns Per Operating Day: 0.9

Shutdown Cause	Frequency
Process water system	14
Gas sensors	11
Improper H_2 piping	4
Software	3
Process water pump failure	1
DC-DC converter failure	1
Unknown	6
TOTAL	40

On June 22 the SPE module was found to be leaking hydrogen into the oxygen system. The module was returned to GE for repairs.

July-November 1984: During this period the module was being repaired. Analysis of the failed module revealed that small particles which apparently had been introduced into the module stack during assembly had perforated the SPE membrane, causing the module failure.

B199
SPE(2)2

December 1984 - July 1985: The new module was reinstalled. From December 4 to July 18 the system was operated in all three modes described above as follows:

Type of operation: Module power weekdays, some nighttime operation
Total number of weekdays: 163
Weekdays with no operation: 80

Cause	Days
GE repairs	3
Process water system	20
Process water pump replacement	27
AC power supply & DC-DC converter repairs	15
Sensor calibration	1
Operation not scheduled	14
TOTAL	80

Weekdays with Operation: 83

Average Hours Per Day: 8.3

Total Number of System Shutdowns: 19

Average Shutdowns Per Operation Day: 0.2

Shutdown Cause	Frequency
Process water system	3
Gas sensors	5
Unknown	11
TOTAL	19

The brief chronology above makes it clear that initial operation was far from smooth. Even after the shakedown was completed, the system was plagued by shutdowns due to malfunctions in sensors, controls, the data acquisition system, and the process water system. However, until the first SPE module failed catastrophically, the PV array, the power supply, and the module itself, i.e. the major system components, all functioned properly and reliably.

Since the second module was installed, there have been some repairs of the process water system and power supply, but none involving sensors (excepting calibration), controls, the data acquisition system, the PV array, or the SPE module itself. The average number of shutdowns per day declined from 0.9 for the first module to 0.2 with the second, while the average operating hours per day rose from 6.2 to 8.3.

The initial difficulties encountered in system operation are felt to be a manifestation of the complex and custom nature of the electrolyzer system.

B199
SPE(2)3

The reduction of these problems as operation continued supports the view that such problems are not intrinsic to the SPE system. However, it is clear from the failure of the first SPE module and the persistence of process water system failures that cleanliness is a paramount concern in the SPE system. These problems add complexity (e.g. in the process water system) and must be dealt with.

2.3 Grid-Powered Electrolyzer Operational Results

Figure 2.1 presents baseline grid-powered electrolyzer operational results. Each baseline consisted of 10 4-hour constant power tests, 2 each at nominal power levels of 3, 6, 9, 12, and 15kW (approximately 200 to 1000 A/ft^2 current density).

The first baseline was conducted with the original SPE module in March 1984. The second and third baselines were conducted with the second module, the second from December 1984 to March 1985, and the third during June and July 1985.

As shown in Figure 2.1, for given current density, the second module performed at a somewhat lower voltage than the first module, especially at high current densities. A slight deterioration in performance (25mV) is evident between the second and third baselines. This translates to a voltage efficiency decrease of about 1%. In Section 2.5 these baseline results are compared to solar-powered and transient simulation results.

2.4 PV-Powered Operational Results

PV Array:

Figures 2.2, 2.3, and 2.4 present PV array performance results. All 3 figures show quadratic least-squared fits of hourly averaged data obtained between December 1984 and July 1985 using the replacement SPE module. Fitting equations, coefficients, standard errors, and standard deviations are all given in Appendix III.

Figure 2.2 presents PV array output power versus solar insolation for the 300% boosted and complementary modes. Both curves are almost perfectly linear with insolation (as one would expect given constant efficiency) and are almost identical.

Figure 2.3, derived from the power output data in Figure 2.2, presents PV array efficiency versus solar insolation for both solar-powered modes. Array efficiency is almost constant at approximately 8% over a wide range of insolations in both cases. The drop in efficiency at low insolation levels represents off-normal and cloudy operating conditions.

Figure 2.4 presents PV array voltage versus solar insolation. Again, both curves are quite similar. The array output voltage (which is controlled by the DC-DC converter discussed below) is almost constant at about 29-30 V, about 8% lower than the nominal 32V maximum power point voltage anticipated.

B199
SPE(2)4

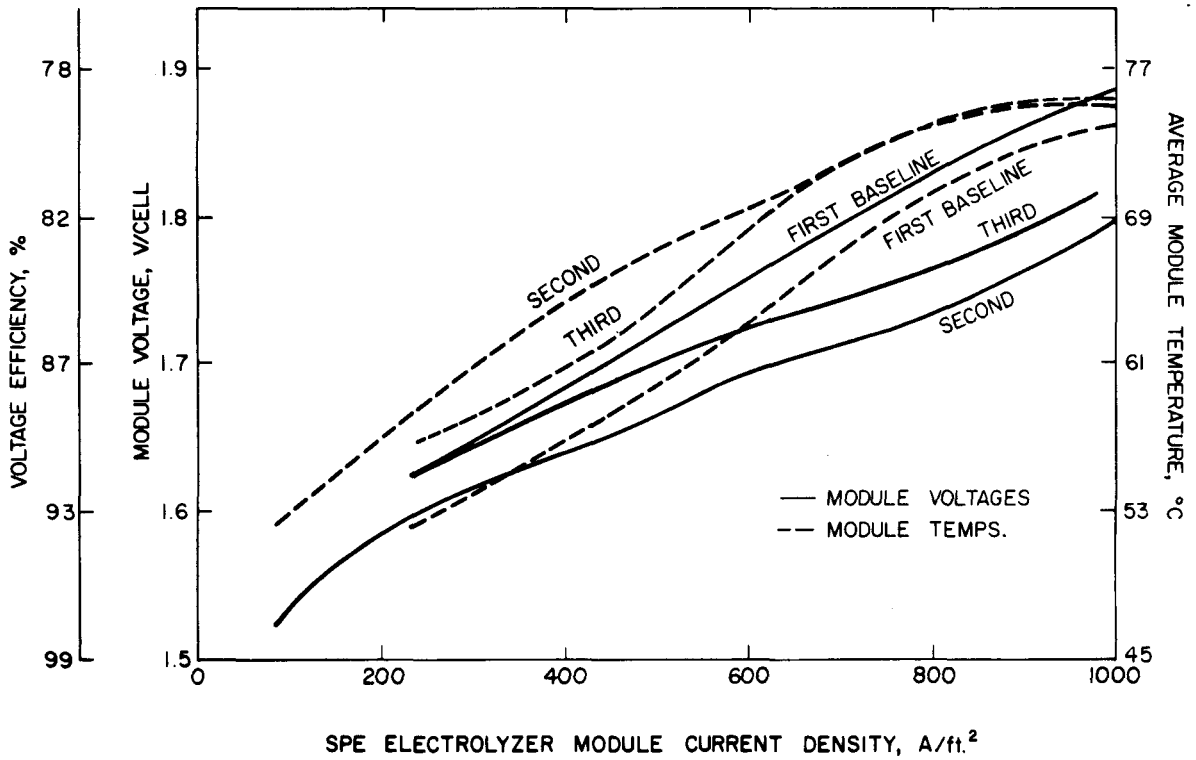

Figure 2.1 Baseline grid-powered electrolyzer operational results. Cell voltage add temperature vs current density.

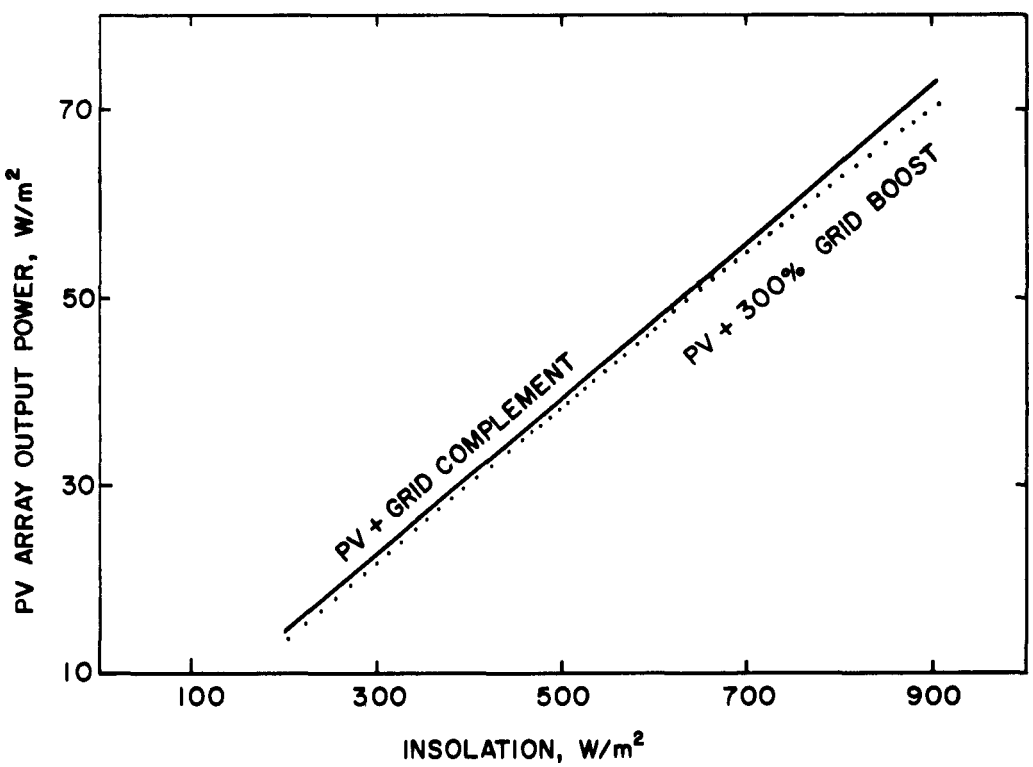

Figure 2.2 PV array output power versus solar insolation.

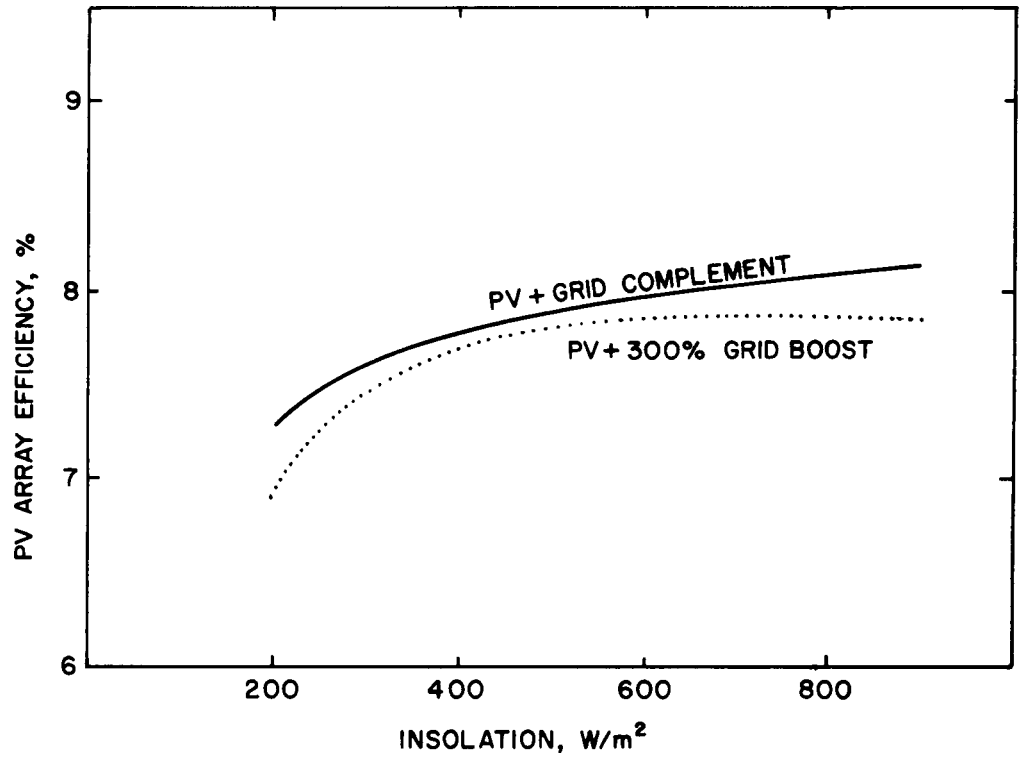

Figure 2.3 PV array efficiency versus solar insolation.

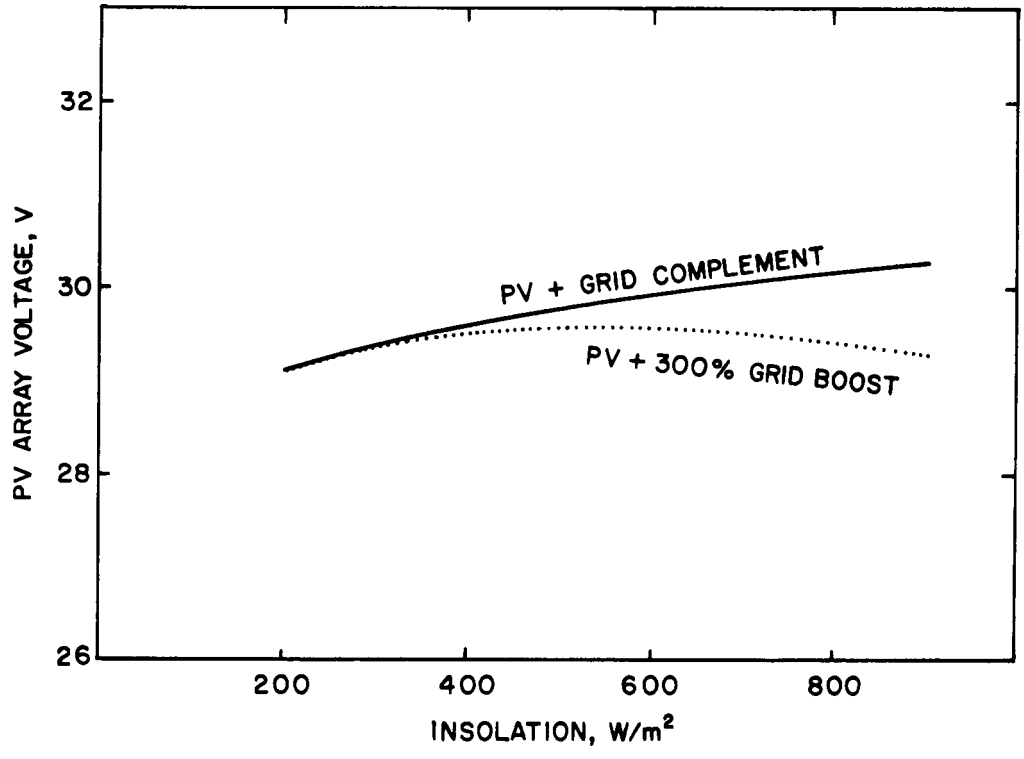

Figure 2.4 PV array voltage versus solar insolation.

Generally speaking the PV array has been extremely reliable, the only failure being a blown fuse. Power output and efficiency results were in line with manufacturer's claims.

DC-DC Converter:

Figures 2.5, 2.6, and 2.7 present quadratic least-squared fits of DC-DC converter results based on hourly averaged data obtained between December 1984 and July 1985 using the replacement module. Fitting equations, coefficients, standard errors, and standard deviations are given in Appendix III.

As shown in Figure 2.5 the converter output power is almost linear with input power, suggesting an almost constant conversion efficiency. The power curves for both solar modes are almost identical.

The DC-DC converter efficiency, shown in Figure 2.6, varies from about 71 to 79%, generally declining as input power rises. The efficiency curves are noticably separated (2%) at low input power levels. The reason for this, as Figure 2.7 indicates, is that the converter output voltages are quite different in the 2 modes. In the 300% boosted mode, low solar insolation translates to low module current and hence to low module voltage (see Figure 2.1). In the complementary mode, module current is constant, i.e. uncorrelated to solar insolation.

The DC-DC converter efficiency, approximately 75%, is seen to be much lower than the 94% needed to match an optimal directly-coupled PV-electrolyzer system (see Appendix I), and much lower than state-of-the-art devices which can achieve efficiencies above 90%.

SPE Electrolyzer:

Figure 2.8 presents quadratic least-squared fits of SPE electrolyzer module voltage versus current and temperature for operation in the 300% boosted PV-powered mode. Results are based on hourly averaged data obtained between December 1984 and July 1985 with the second module. The fitting equation, coefficients, standard errors, and standard deviations are given in Appendix III.

Results are presented for temperatures between 60°C and 75°C, the normal range of module operating temperatures. The data has been grouped into 5°C temperature bins. As Figure 2.8 shows, module voltage declines with rising temperature and rises with rising current density. The voltage-current density functionality is quite similar to that found in the baseline case as shown in Figure 2.1 and discussed in Section 2.5.

Typical System Operation:

Figure 2.9 is an hourly system energy histogram for operation in the 300% boosted PV-powered mode on a typical day (July 17, 1985). For each hour, the

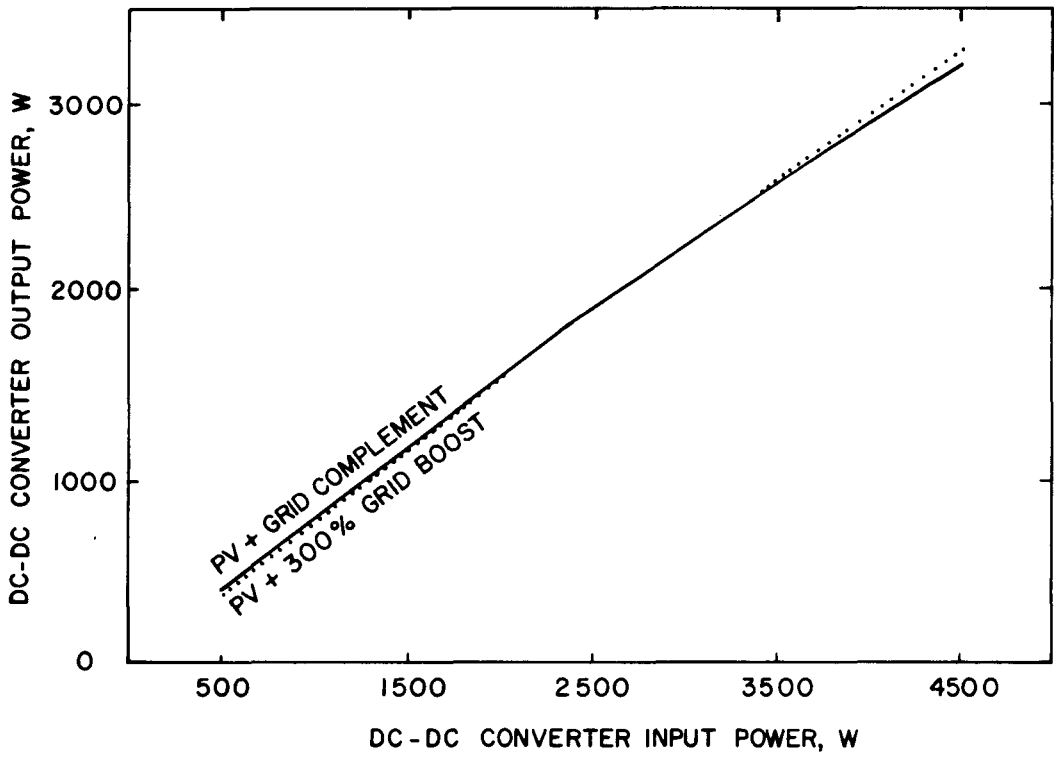

Figure 2.5 DC-DC converter output power versus input power.

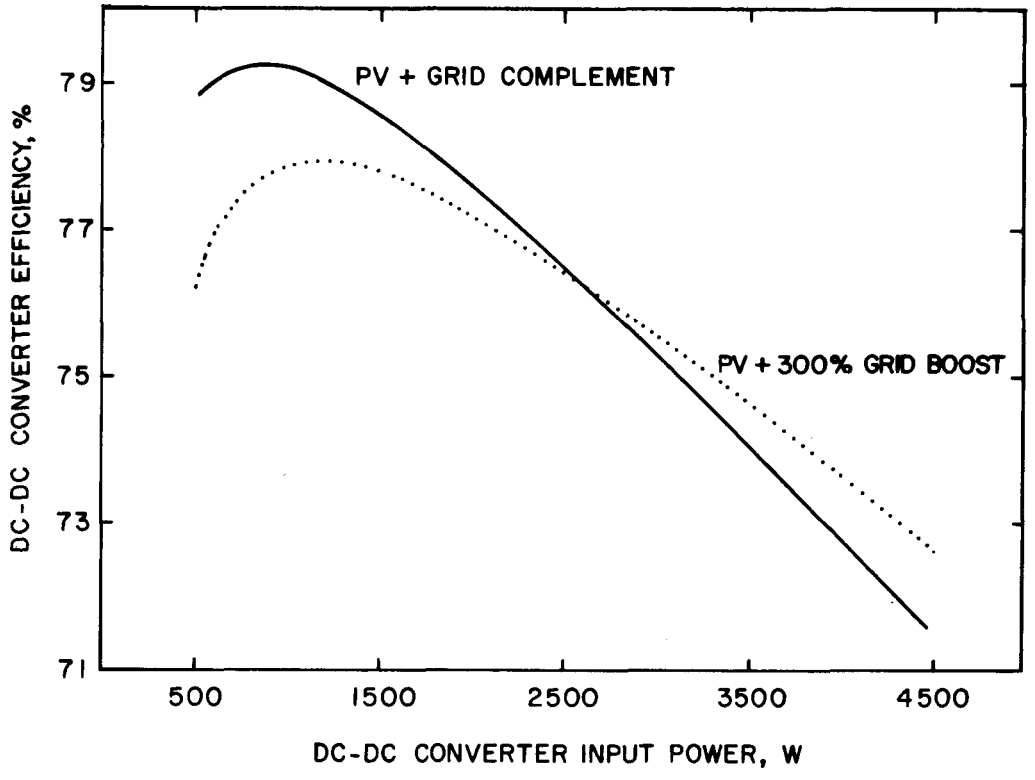

Figure 2.6 DC-DC converter efficiency versus input power.

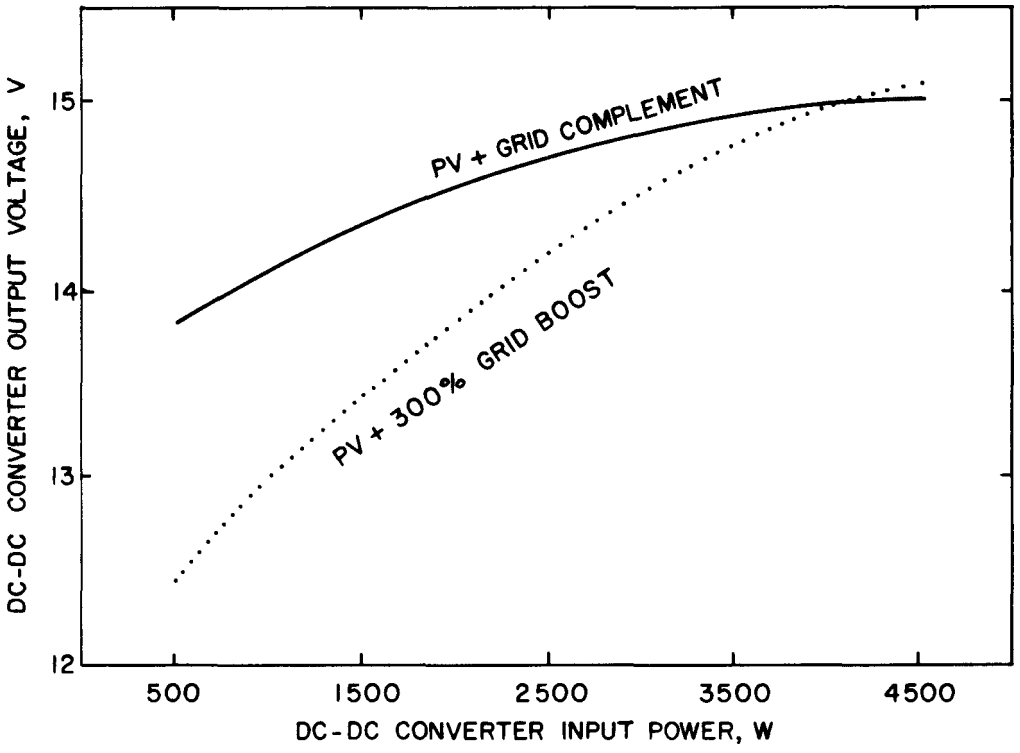

Figure 2.7 DC-DC converter output voltage versus input power.

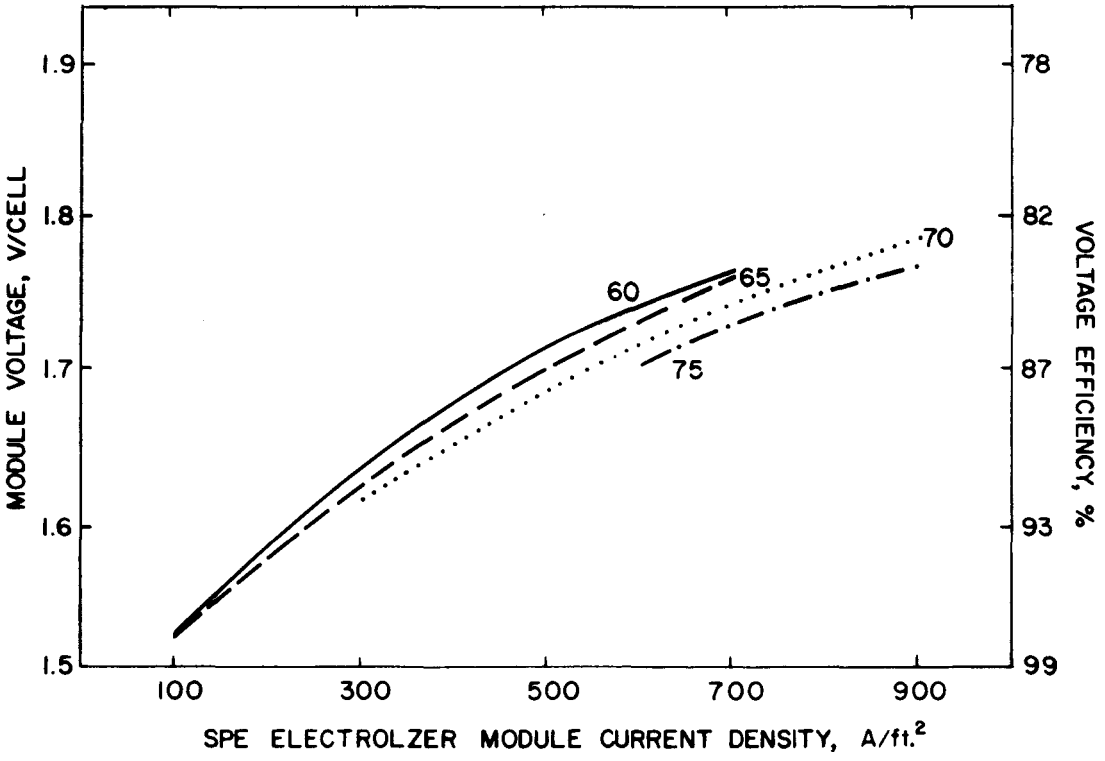

Figure 2.8 SPE electrolyzer module voltage versus current density and temperature for 300% boosted PV-powered operation.

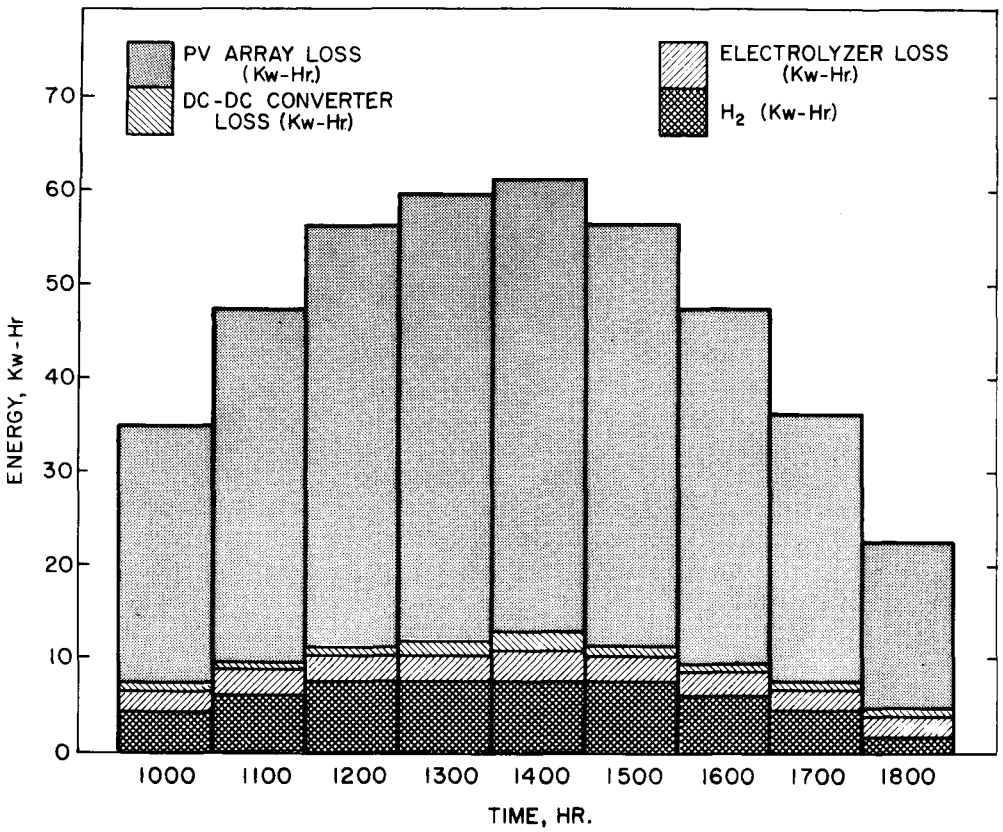

Figure 2.9 Typical hourly system energy histogram in 300% boosted PV-powered operation (July 17, 1985).

total band height is the total energy entering the system. For example, for the hour ending at 14:00, the solar insolation incident on the PV array was 53.1 kWH while the power supply contributed 8.3 kWH, for a total of 61.4 kWH.

The top portion of each band represents the unused solar insolation--for 14:00 49.2 kWH, or 93% of the incident insolation. The next section of band is the energy loss in the DC-DC converter, usually about 25% of its input power. The third portion of band represents all electrolyzer-related losses, both voltage efficiency (typically 10-20%) and dryer losses (roughly 10%). The lowest portion represents the energy constant of the hydrogen produced, at 14:00 7.9 kWH.

Figure 2.10 presents some component efficiencies for this same operating day. The electrolyzer voltage efficiency is quite stable at about 80-85%, declining in midday when the solar insolation and module current is highest. The DC-DC converter efficiency, averaging roughly 75%, behaves similarly. The PV array efficiency is steady throughout the day at 7-8%.

2.5 Comparison of Baseline, PV-Powered and Transient Simulation Results

Three important issues have arisen during the course of this work:

- Validity of the computer simulation module presented in Appendix I.
- Performance stability of the SPE module.
- Relationship between baseline steady-state test results and solar-powered transient test results.

In order to resolve these issues, Table 2.1 compares baseline and 300% boosted PV-powered tests results with computer simulation results presented in Appendix I.

As Table 2.1 shows the voltage efficiency obtained from the computer simulation results is very close (within 1%) to the first baseline test results (obtained using the first module). The simulation model predicts slightly lower efficiency (1-4%) than baselines 2 and 3, obtained with the second module. The simulation results compare similarly with the 300% boosted PV-powered test results, obtained with the second module.

Thus, the simulation model correctly predicts module voltage efficiency within 4% for all cases, and is valid to this level of accuracy. The model, based on manufacturer's data, consistently under-predicts voltage efficiency slightly, especially at high current densities.

Comparison of baseline tests 2 and 3 (both obtained with module 2) show a slight but noticeable decline (about 1%) in voltage efficiency over a period of a few months. Module temperatures are quite similar in both tests.

B199
SPE(2)6

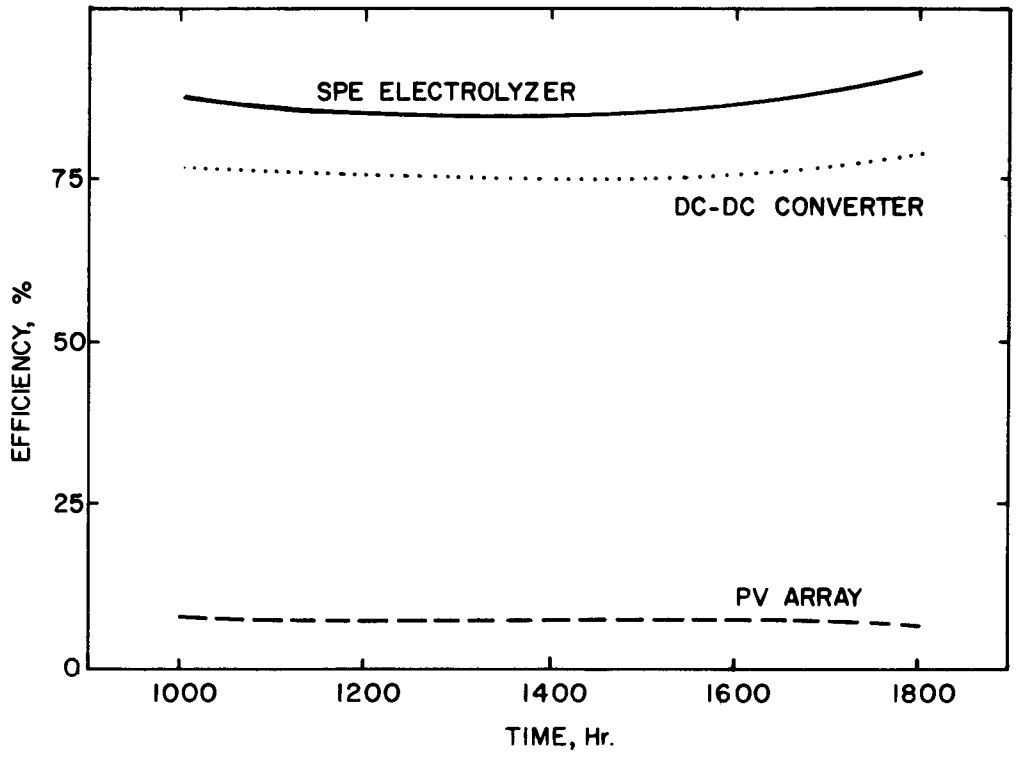

Figure 2.10 Typical hourly system efficiencies in 300% boosted PV-powered operation (July 17, 1985).

Table 2.1
Comparison of Module Cell Voltages and Voltage Efficiencies for Baseline Tests, 300% Boosted PV-Powered Tests, and Computer Simulation Model

					Cell Voltage (V)			Cell Voltage Efficiency (%)		
Baseline Test #	Baseline Module #	Nominal Baseline Test Power Level (kW)	Module Temp. (°C)	Module Current Density (A/ft^2)	Baseline (Fig. 2.1)	300%* Boosted (Fig. 2.8)	Computer** Simulation (Eq. I-1)	Baseline	300%* Boosted	Computer** Simulation
1	1	3	52	231	1.63	NA	1.63	91	—	91
		6	58	443	1.70	1.69	1.72	87	88	86
		9	65	642	1.78	1.75	1.79	83	85	83
		12	71	823	1.84	1.77	1.83	80	84	81
		15	74	994	1.89	1.78	1.87	78	83	79
2	2	1	53	82	1.53	NA	1.55	97	—	95
		3	58	235	1.60	1.60	1.61	93	93	92
		6	66	456	1.65	1.69	1.70	90	88	87
		9	71	664	1.71	1.73	1.77	87	86	84
		10	72	732	1.72	1.75	1.79	86	85	83
		12	75	862	1.75	1.76	1.83	85	84	81
		14	75	1003	1.79	1.78	1.87	83	83	79
3	2	3	57	233	1.62	NA	1.62	91	—	91
		6	62	448	1.69	1.70	1.71	88	87	87
		9	70	656	1.73	1.72	1.77	86	86	84
		12	75	853	1.76	1.76	1.82	84	84	81
		14	75	974	1.81	1.78	1.86	82	83	80

* Module #2
**Based on manufacturer's data.
NA=Not Available.

B199
SPE(2)8

Comparison of baseline tests 2 and 3 with 300% boosted PV-powered test results shows very little difference in electrolyzer efficiency (0-2%). No consistent pattern is evident. Thus, according to these test results, electrolyzer performance is unaffected by transient solar-powered operation.

B199
SPE(2)7

3.0 TECHNOECONOMIC ANALYSIS

This section presents the results of a parametric analysis of electrolytic hydrogen costs for both grid- and PV-powered operation. These results are followed by an economic comparison to natural gas reformer hydrogen production.

3.1 Parametric Hydrogen Cost Analysis

This section presents the results of a parametric analysis of electrolytic hydrogen costs. The results were obtained using the economic model described in Appendix II which is based in part on the computer transient simulation results presented in Appendix I, and validated by comparison with actual operational results in Section 2.

Operating Modes Considered

Three operating modes have been analyzed using the model:

- Grid-Powered Electrolyzer Operation
- Stand-Alone PV-Powered Operation
- PV Supplemented by 8 Hour/Day Off-Peak Grid Electricity

In the grid-powered operating mode, the electrolyzer operates round the clock, 8766 hours/year, subject to an electrolyzer availability factor to account for downtime from maintenance and breakdowns. In the stand-alone PV-powered operating mode, all electricity used to produce hydrogen is derived from the PV array. System performance in this mode is determined from computer transient simulation results described in Appendix I, and validated in Section 2. The third mode, PV supplemented by 8 hour/day off-peak grid electricity, seeks to better utilize the electrolyzer--the stand-alone PV-powered system will operate at most 8-10 hours/day--while also reducing the cost of purchased electricity. Ancillary power requirements are not considered in any mode.

Fixed Parameters

A number of parameters were held fixed throughout the analysis. These quantities and the values selected are presented in Table 3-1.

Other Assumptions

Depreciation, income tax effects, and inflation are not considered. Electricity purchases (grid-operation) and sales (PV-operation) are both made at the same price, assumed constant throughout the system lifetime. All PV-powered results are based on the computer transient simulation results presented in Appendix I, which were derived using New York City weather data. The electrolyzer is assumed to operate at 80°C in all modes.

B199
SPE(3)1

Table 3-1
Fixed Electrolyzer System Parameters

Quantity	Value
Operating and Maintenance Cost Expense	2% of total installed capital cost/year
Property Tax Expense	2% of total installed capital cost/year
System Lifetime	20 Years
Salvage Value	0
Discount Rate	10%
Electrolyzer Availability (Fraction of time system is available for use)*	90%

*Applies to grid-powered operation only.

Free Parameters

Using the model described in Appendix I, the annualized hydrogen production cost was computed for all three modes cited above. The analysis was conducted parametrically in terms of the quantities listed in Table 3-2 in order to determine the sensitivity of hydrogen cost to each of these parameters.

Results

Grid Powered Electrolyzer Operation

Figure 3.1 presents hydrogen production cost for grid-powered operation as a function of electricity cost, electrolyzer installed capital cost and electrolyzer capacity utilization/efficiency. Results are presented for both a 100% utilization of the SPE electrolyzer module (1050 A/ft^2 current density and 83% efficiency) and a 50% utilization (525 A/ft^2 current density and 92% efficiency) in order to examine the tradeoffs between electrolyzer capital cost and efficiency.

As Figure 3.1 shows, hydrogen cost is very sensitive to electricity cost, electrolyzer capital cost, and utilization. Only for the lowest electrolyzer capital cost ($300/kWe) is it desirable to operate the electrolyzer at a lower current density in order to increase operating efficiency and then only at electricity costs above 5¢/kWh.

B199
SPE(3)2

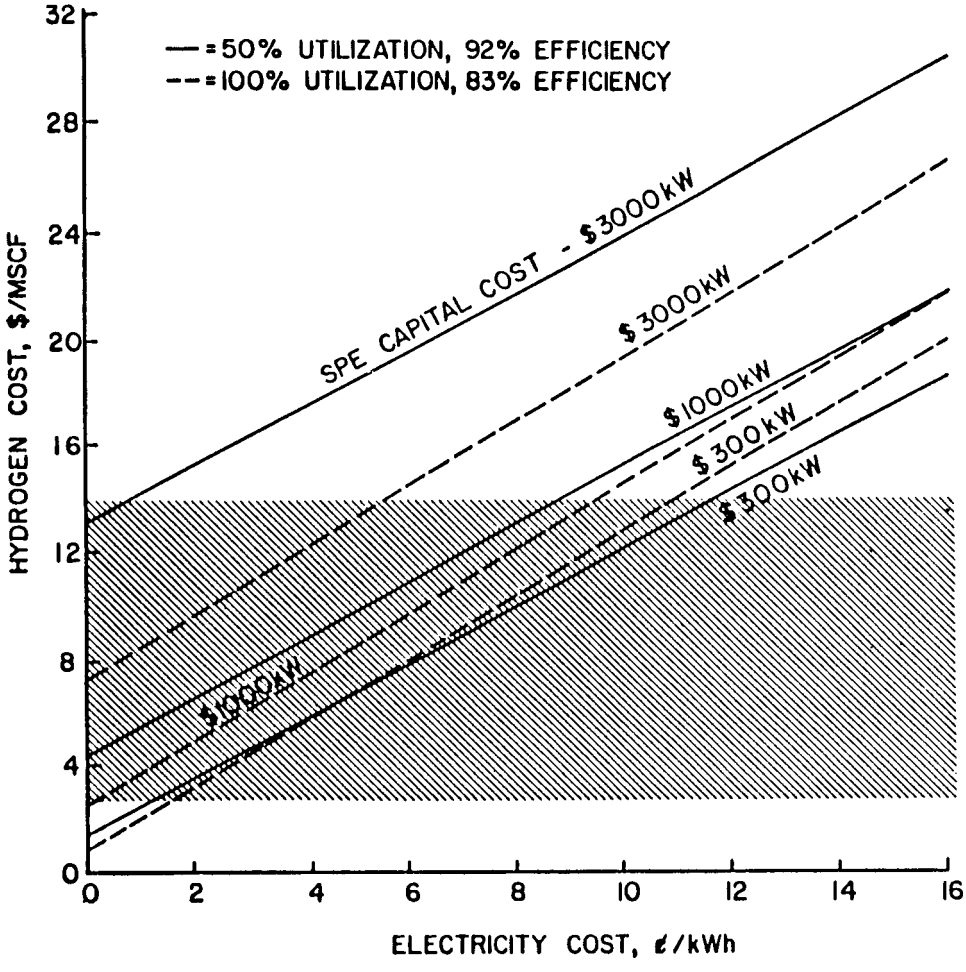

Figure 3.1 Hydrogen cost vs electricity cost, electrolyzer installed capital cost, and capacity utilization for grid-powered electrolyzer operation.

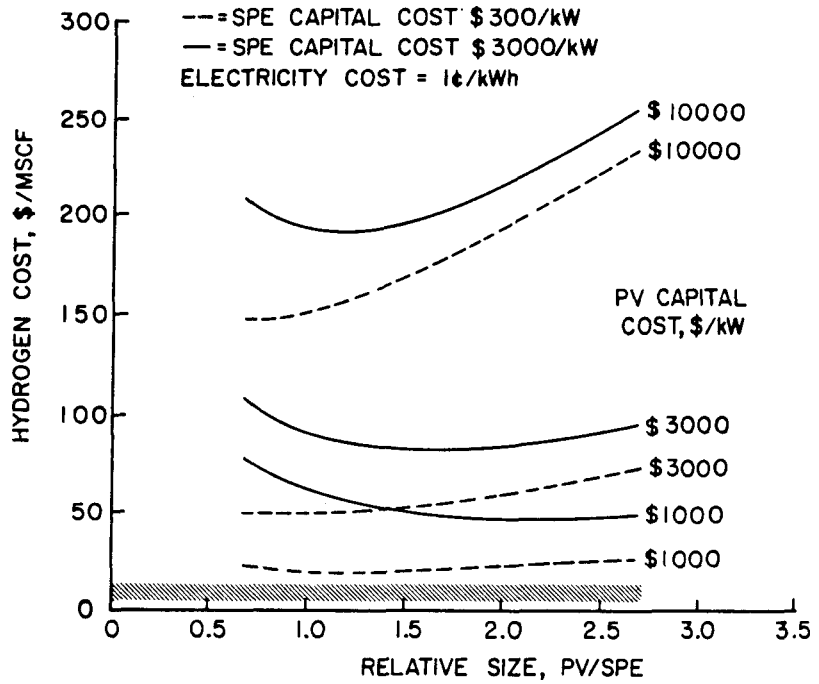

Figure 3.2 Hydrogen cost vs relative PV array/electrolyzer size, PV capital cost, and electrolyzer capital cost for stand-alone PV-powered operation. Electricity cost 1¢/kWh.

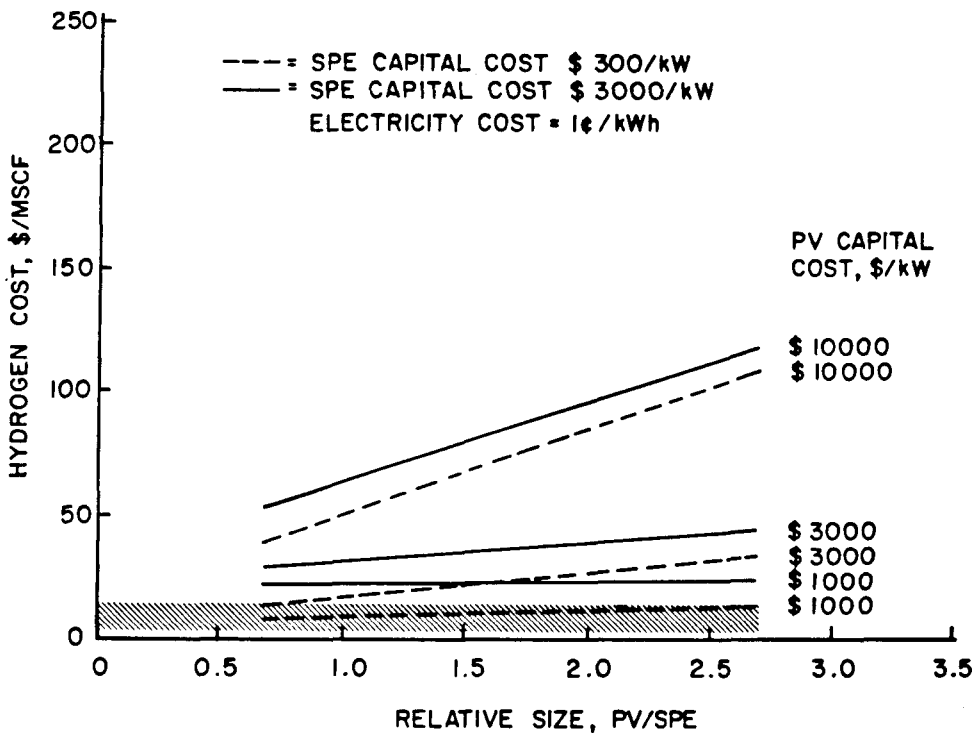

Figure 3.3 Hydrogen cost vs relative PV array/electrolyzer size, PV capital cost, and electrolyzer capital cost for PV supplemented by 8-hour/day off-peak grid operation. Electricity cost 1¢/kWh.

Table 3-2
Quantities Treated Parametrically in Economic Analysis

Quantity	Units	Values
Electrolyzer Installed Capital Cost	$/kWe	300, 1000, 3000
PV Array Installed Capital Cost	$/kW peak	1000, 3000, 10,000
Electricity Cost	¢/kWh	1, 3, 10
Relative Nominal Size PV Array/Electrolyzer	None	0, 0.67, 1.33, 2.00 2.67, 3.33
Electrolyzer Capacity* Utilization (Maximum current/ maximum current possible)	%	100, 50
Electrolyzer Efficiency*	%	83, 92

*Applies to grid-powered operation only; efficiencies are computed using Equation I-1, assuming current densities of 1050 and 525 A/ft^2, respectively.

Stand-Alone PV-Powered Operation

Figure 3.2 presents hydrogen cost for stand-alone PV-powered operation versus relative PV array/electrolyzer size, PV capital cost, and electrolyzer capital cost, for an electricity cost of 1¢/kWh. Hydrogen costs are far higher than those shown in Figure 3.1 for grid-powered operation, except for cases of very high electricity cost and low PV array prices.

As Figure 3.2 shows, for high capital cost electrolyzers ($3000/kWe), PV-powered electrolysis systems are optimal--lowest cost hydrogen--with substantial relative array sizes. For low capital cost electrolyzers ($300/kWe), no such optimum size exists (above 0.67) unless the PV array is very inexpensive ($1000/kW peak). In all cases hydrogen cost is very sensitive to PV array and electrolyzer capital costs. Hydrogen cost is quite insensitive to electricity cost because electricity sales are minimal (see Table II-3).

PV Supplemented by 8 Hour/Day Off-Peak Grid Electricity

Figures 3.3 and 3.4 present hydrogen cost for PV supplemented by 8 hour/day off-peak grid electricity operation versus relative PV/electrolyzer size, PV capital cost, electrolyzer capital cost, and grid electricity cost. For any given set of capital costs, the resulting hydrogen cost is intermediate between those found in Figure 3.1 for grid-powered operation and in Figure 3.2 for stand-alone PV-powered operation. This occurs because grid electricity

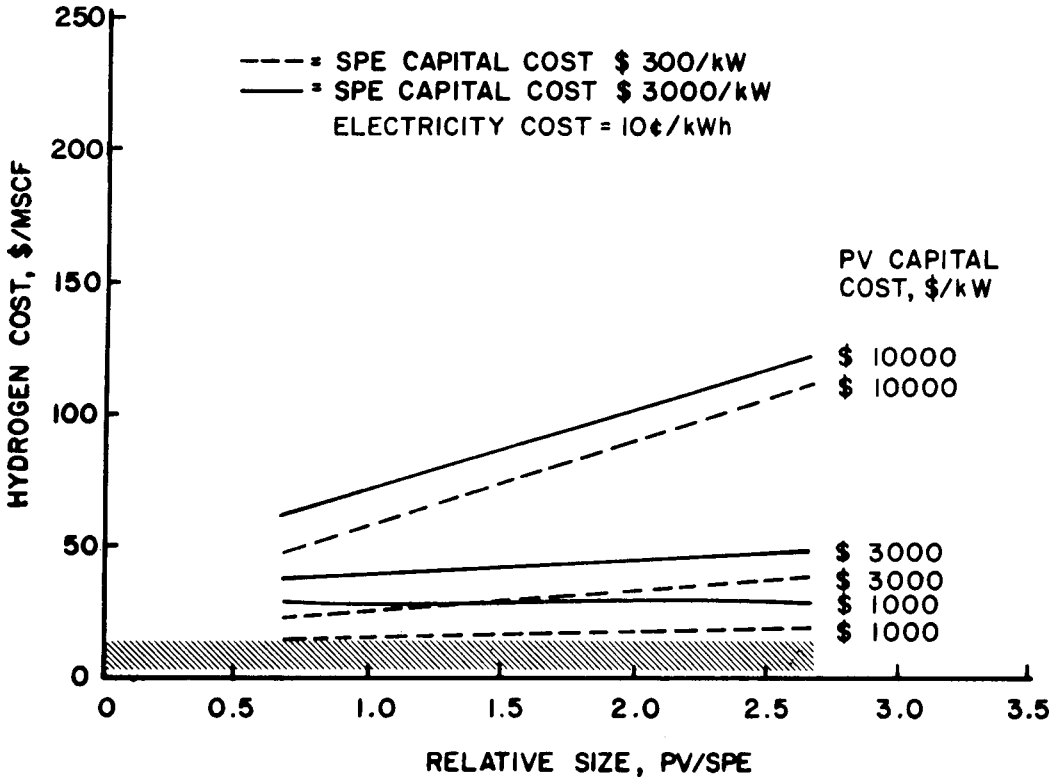

Figure 3.4 Hydrogen cost vs relative PV array/electrolyzer size, PV capital cost, and electrolyzer capital cost for PV supplemented by 8-hour/day off-peak grid operation. Electricity cost 10¢/kWh.

costs are almost always lower than the annualized cost to produce electricity with a PV array, plus much better utilization of the electrolyzer capacity.

No optimal relative PV array size (above 0.67) exists for the combined system except for the combination of lowest cost PV array ($1000/kW) and highest cost electrolyzer ($3000/kWe), where a very shallow minimum occurs for both values of electricity cost (1¢ and 10¢/kWh). Thus--except for this case --the minimum hydrogen cost is obtained by minimizing the relative size of the PV array.

An important feature of Figures 3.3 and 3.4 is that hydrogen cost is quite insensitive to PV array relative size except at the highest PV array cost ($10,000/kW peak). The reason for this is that the use of grid electricity "buffers" the impact of PV cost on hydrogen production cost, i.e., grid electricity substitutes for more expensive PV electricity.

The converse of this statement--that the PV array buffers the impact of increasing electricity costs--is also true, as can be seen by comparing Figures 3.3 (1¢/kWh) and 3.4 (10¢/kWh) for a given set of capital costs. The upshot of this observation is that, although PV-produced hydrogen is costly today, PV arrays might be considered in a "hedging" strategy to reduce the impact and risk of increasing electricity cost.

General Conclusions

Given the assumption made here, of the three options studied, the grid-powered system produced the least costly hydrogen--usually by a wide margin, followed by the combined system, and then by the stand-alone PV system. For the two PV cases, the economic model developed in Appendix II can be used to determine the optimal relative PV array size. It also appears that, although costly today, PV electricity reduces the impact of future grid electricity cost increases.

3.2 Comparison to Natural Gas Reforming

Figures 3.1 to 3.4 each contain a shaded band which represents the range of 1985 projected hydrogen production costs using a natural gas reformer ($2.89-14.40/MSCF in 1984 dollars).[1] As Figure 3.1 shows, a grid-powered system can compete with these costs over a wide range of electricity costs if the electrolyzer capital cost is low enough or with a high electrolyzer cost if electricity is very low cost.

Figure 3.2 shows that the stand-alone PV-powered system cannot compete under even the lowest capital cost assumptions. As shown in Figures 3.3 and 3.4, the combined system is marginally competitive, i.e., if capital costs are quite low. In this case, the sensitivity to electricity cost is low, as discussed above.

B199
SPE(3) 4

4.0 SUMMARY AND CONCLUSIONS

This report represents the completion of the first major evaluation at the BNL Hydrogen Technology Evaluation Center. The PV-powered electrolyzer system and data acquisition/control system were operated to measure component performance, to validate a computer simulation model of the system, and to examine the economics of such systems.

Steady-state baseline tests were conducted using grid power. PV-powered operation was performed in a 300% boosted mode and in a complementary mode with grid.

A chronology of operation has been developed. The first SPE module failed after a few months of operation. Other problems related to the complexity of the system were gradually solved as operation continued.

Two computer models have been developed. A technical model performs transient simulations of PV-powered electrolyzer systems. An economic model, using simple assumptions, computes the annualized cost to produce hydrogen via electrolysis, based on the simulation model results.

A comparison of results shows that the electrolyzer transient simulation model developed coincides closely with observed electrolyzer performance. Further, test results show little difference between steady-state baseline module performance and transient solar behavior.

Economically, a grid-powered electrolyzer can compete with natural gas reformer-derived hydrogen if electrolyzer capital cost is low. A stand-alone PV-powered system cannot, due to the high cost of PV-derived electricity and poor electrolyzer capital utilization. A combined PV-grid system is marginal, and can provide a hedge against future electricity price increases.

B199
SPE(4)1

REFERENCES

1. The Futures Group, "The Market Potential for Electrolytic Hydrogen," EPRI EM-1154 (August 1979).

B199
SPE(R)1

APPENDIX I

PHOTOVOLTAIC-ELECTROLYZER SYSTEM TRANSIENT SIMULATION RESULTS

(Formerly published by R.W. Leigh, P.D. Metz, and K. Michalek as BNL 34081, December 1983)

ABSTRACT

This appendix presents transient simulation results for the PV-powered electrolyzer system described in the body of this report. Innovative features of the modeling include the use of real weather data, detailed hourly modeling of the thermal characteristics of the PV array and of system control strategies, and examination of systems over a wide range of power and voltage ratings. The transient simulation system TRNSYS was used, incorporating existing, modified or new component subroutines as required. For directly coupled systems, we found the PV array voltage which maximizes hydrogen production to be quite near the nominal electrolyzer voltage for a wide range of PV array powers. The array voltage which maximizes excess electricity production is slightly higher. The use of an ideal (100% efficient) maximum power tracking system provides only a six percent increase in annual hydrogen production. An examination of the effect of PV array tilt indicates, as expected, that annual hydrogen production is insensitive to tilt angle within $\pm$ 20° of latitude. Summer production greatly exceeds winter generation. Tilting the array, even to 90°, produces no significant increase in winter hydrogen production.

I-A. Introduction

The technical approach adopted to evaluate the PV-powered electrolyzer system is a coordinated program of system testing, computer simulation, and economic analysis. This appendix presents the computer simulation results of the PV-electrolyzer system, described in the body of the report and elsewhere,[1,2] one of the largest and most advanced ever evaluated.[3-6] Section I-B outlines the computer simulation approach used. Section I-C presents the component models and operating modes of the simulation program developed. Section I-D presents the simulation results.

I-B. Simulation Approach

Simulation techniques provide the most accurate non-experimental estimates of the performance of solar energy systems. Simulation is especially important for solar energy systems, with their stochastically varying energy source, and for systems such as the electrolyzer considered here where the efficiencies are functions of the operating conditions. For a novel system such as this one where sizing decisions cannot be based on experience, simulation offers a method for testing the effects of various decisions in advance of construction.

Therefore, we present simulation results below for the annual hydrogen production of the PV-electrolyzer system for a wide range of PV array sizes, for various possible wiring arrangements, and for operation with and without a control system for maximum power tracking of the PV array. The results offer valuable design guidelines in their own right, and will serve as the basis of economic analysis to be reported elsewhere.

B199
SPE(A/I)2

Our simulations build on existing work by others. Carpetis[5] constructed a simulation model of a photovoltaic powered electrolyzer which included detailed treatment of the electronic interactions; the array temperature, however, was entered exogenously rather than calculated from the assumed weather patterns. We will compare his results for Frieberg (West Germany) with ours for New York (USA) when appropriate. Freudenberg[7] created a hybrid simulator based on actual solar cells and an electronic load with characteristics representing an electrolysis cell. He found the PV characteristics to be well matched to the assumed electrolyzer voltage-current curve for the six month period during which he took data. These efforts stimulated our interest in examining a large number of potential systems and in representing additional significant details of the systems in our models.

For simplicity in constructing the simulation model for the photovoltaic-powered electrolyzer, we considered a system powered exclusively by the PV array. The amount of excess PV energy which could be sold to the electric utility is calculated. The behavior of a system in which the electrolyzer runs at all times, using grid-supplied electricity when PV power is not available, may be derived from these data.

I-C. The Simulation Program

The model was structured around TRNSYS, a well known solar energy simulation system[8] and uses hourly weather data for the "typical meteorological year" for New York City produced by the SOLMET program.[9] The configuration of the simulation system is shown in Figure I-1. The structure of the individual components and the operating modes of the program are discussed below.

I-C.1 Program Operation

As illustrated in Figure I-1, for each hour in which there is sufficient insolation to operate the system, the PV thermal model calculates the cell temperature, and the PV electrical model calculates the power output of the PV array at a given voltage (or the maximum power in the maximum power tracking mode; see Section I-C.4). Then the electrolyzer model, using this value for power, calculates the voltage at which the electrolyzer would operate. This voltage is then used as data by the PV electrical model, and an iterative process finds values of power and voltage for which the characteristics of both the PV array and the electrolyzer are simultaneously satisfied. Hourly electricity and hydrogen production are accumulated to generate monthly and annual totals. Hourly values of all quantities are available as desired for validation or analysis.

I-C.2 Component Model-Photovoltaics

Our version of TRNSYS (10.1) did not include subroutines which would represent PV modules. Although component subroutines to represent PV modules have been developed at the University of Arizona and included in later versions of TRNSYS[10], we chose to use comparable models developed at MIT[11,12] which were available with parameters describing appropriate PV cells and with detailed experimental validation of those parameters.

B199
SPE(A/I)3

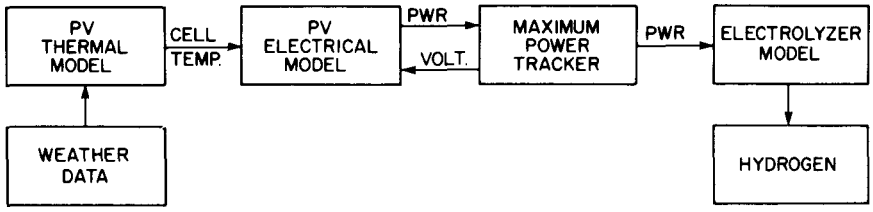

(a)

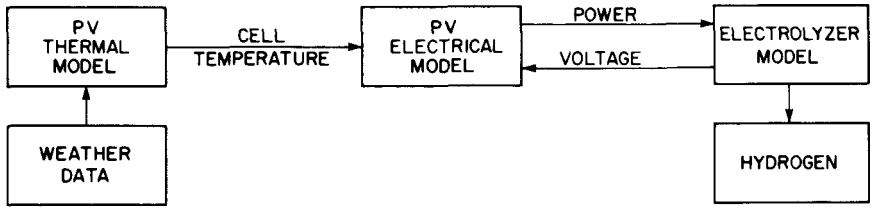

(b)

Figure I-1. Simulation system for maximum power tracking (a); and direct coupling (b).

The thermal model, calculates the module temperature using a small number of empirical constants. With no wind, the module is assumed to stabilize at a temperature which exceeds ambient by an amount proportional to the total insolation; three more constants describe a simple exponential variation in wind-induced cooling. Finally, since these considerations result in an estimate of an equilibrium temperature for a given set of climatic conditions, a time constant representing the thermal mass of the modules describes the approach of the modules to this equilibrium temperature from the temperature of the previous time interval.

Thermal loss coefficients of 0.010, 0.005, and 0.002°C/(kJ/m2-hr) at 0 and 5 m/sec and "very large" windspeeds, respectively, gave temperature variations in good agreement with those reported in Reference 11 for arrays comparable to ours. The 15-minute time constant for our arrays meant that dynamic effects were negligible in our current approximation of hourly modeling. As operational data on our system becomes available, these values will be refined.

The electrical characteristics of the PV modules were simulated using a subroutine adapted from one written by the MIT group,[12] based on algorithms developed elsewhere.[13,14] These represent the electrical characteristics of the solar cell by the equations describing a current source proportional to the insolation, a diode with an exponential characteristic curve in parallel to the current source and a series resistance on the output. Four constants

B199
SPE(A/I)4

thus describe the characteristic I-V (current-voltage) curve of the modules at a reference insolation and temperature. Three more constants, and the reference temperature and insolation, describe the translation of this characteristic curve in the I-V plane under the influence of varying temperature and insolation. Constants experimentally determined at MIT for Solarex cells[12] were used for all simulations. All of these constants were appropriately scaled to represent arrays of differing peak powers or the various series-parallel wiring options that give arrays of differing voltage for the same peak power.

I-C.3 Component Model-Electrolyzer

Carpetis[5] has prepared two models of solid polymer electrolyzers, one based on a linear current-voltage relationship, the other giving the voltage as a fourth order polynomial in the current. We found an intermediate approach optimal: quadratic fits to experimental data on the electric input power[15] and temperature[16] dependence of the electrolyzer voltage gave, for a single cell voltage V, the expression

$$V = V_0 \left[1+A_1P\ (1-A_2P)\right] \left[1-B_1T\ (1-B_2T)\right] \qquad (I\text{-}1)$$

where P is the electrical power in W/ft^2, T is the Celsius temperature, and V_0, A_1, A_2, B_1, and B_2 are empirical constants given in Table I-1. The model was constructed to permit arbitrary series and parallel arrangements of multiple cells, but for these runs always had 8 cells in series. The electrolyzer current was limited to 1.08×10^4 A/m^2 (1000 A/ft^2) with excess power presumed to be sold elsewhere. Hydrogen production was calculated (as is found experimentally[15]) assuming 10% losses due to coulombic inefficiency and gas dryer purging.

I-C.4 Operating Modes

As illustrated in Figure I-1, two different modes of operation of the model are possible. In the maximum power tracking mode (Fig. I-1a), an iterative search internal to the PV array subroutine finds the point on the V-I curve giving maximum power output. The maximum power tracker model provides this power--minus a preselected fractional parasitic loss attributed to the power tracker--to the electrolyzer model. The voltage signal from the electrolyzer model is ignored. In this paper, simulation results are presented for an ideal (100%) efficient MPT device, and for a more realistic device assumed to have parasitic losses of 10%, i.e., 90% efficient.

Table 1
Electrolyzer Model Constants

Constant	Value
V_0 (Volts)	1.7316
A_1 (m^2/W)	2.232×10^{-5}
A_2 (m^2/W)	1.686×10^{-5}
B_1 ($^oC^{-1}$)	3.0149×10^{-3}
B_2 ($^oC^{-1}$)	3.3400×10^{-3}

B199
SPE(A/I)5

In the directly coupled mode (Fig. I-1b), the array is wired directly to the electrolyzer; wiring losses are assumed negligible, and the voltage level derived in the electrolyzer determines the point on the V-I curve, and thus the current and power produced by the array. Simulation results for both operating modes are presented in Section I-D.

I-C.5 Convergence of Simulations

In the maximum power tracking mode, operation of the system was straightforward; weather conditions would determine the maximum PV cell output, and the available power would be fed into the electrolyzer. The electrolyzer model then found a voltage consistent with the power input, the current equal to power divided by voltage, and the consequent hydrogen production.

In contrast, the directly coupled mode of operation requires an iterative solution, since the PV model can only calculate a power output for a given voltage input, and the electrolyzer model can only find the operating voltage if it has a given power input. TRNSYS has built into it an iterative process for dealing with such situations, but in practice, this did not always converge, due to the particular geometry of the curves representing the PV and electrolyzer characteristics.

We therefore constructed an extra TRNSYS component which gathered data from two iterations, constructed linear approximations to the characteristic curves of the PV array and the electrolyzer and solved for the point of intersection of these curves. This system converged rapidly for all but a few pathological cases which proved unimportant to the analysis; similar convergence aids have been written by others.[17]

I-D. Results of System Simulations

To determine optimal array sizes and configurations for the eight-cell, 15 kW (nominal) electrolyzer, we simulated the operation of a large number of possible systems. We begin with a discussion of the maximum power tracking system and then move to directly coupled systems, concluding with a comparison of the two.

I-D.1 Maximum Power Tracking System Hydrogen Production

Annual hydrogen production results for a series of 90% efficient MPT runs at various array sizes (peak powers) are shown as "x"s in Figure I-2 and are listed in Table I-2. For small array sizes, all the energy produced by a small increase in array size is converted to hydrogen, and annual production increases linearly with array size. For larger arrays the peak power of the array exceeds the peak capacity of the electrolyzer and some of the PV-produced electricity must either be discarded or sold; in either event it does not contribute to hydrogen production which then increases more slowly with array size. For arbitrarily large arrays, hydrogen production saturates at an amount equal to the electrolyzer output capacity multiplied by the number of hours per year for which insolation is sufficient to turn on the system. This value, 8.56 million liters per year, is in good agreement with the apparent asymptote in Figure I-2.

B199
SPE 6

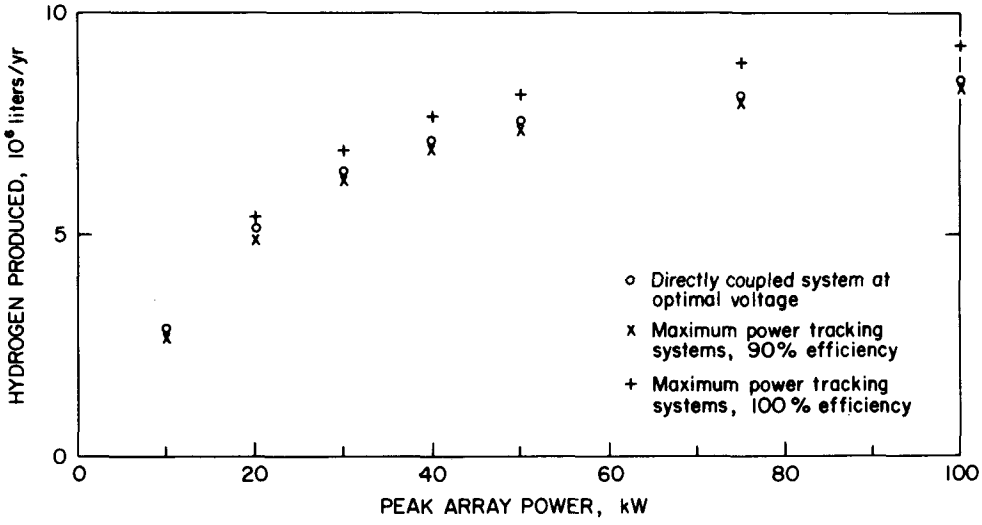

Figure I-2. Hydrogen production vs array size.

I-D.2 Maximum Power Tracking System Electricity Production

PV arrays with peak power in excess of 20 kW produce significant amounts of electricity that cannot be used by the electrolyzer; this electricity could be sold to the local utility or used for some other purpose. In selecting an economically optimal system, its value must be taken into account. Table I-2 indicates the amount of DC electricity available for sale or other use. Losses associated with the conversion to AC would be important in the case of sale to the utility.

I-D.3 Maximum Power Tracking System Dependence on Tilt Angle

A free-standing PV array such as ours can be tilted at any desired angle. Two competing considerations are the desire to maximize annual hydrogen production from the system and the desire to have a production rate that is as uniform as possible during the course of the year, due to the high expenses associated with annual storage.

We simulated the performance of a 10 kW array at several tilt angles and, as expected (18,19), found annual production to be quite insensitive to tilt angle over a broad range around the latitude: 2.65, 2.68, 2.65, and 2.58 million liters at 20, 30, 40, and 50 degrees, respectively. Production did

Table I-2
Annual Hydrogen and Excess Electricity Production for MPT
And for Optimal Hydrogen Producing Directly Coupled Systems

Nominal Peak Power Array (kW)	Annual Hydrogen Production (10^6 l)			Excess DC Electricity (MWh)		Optimal Hydrogen Prod. Voltage For Directly Coupled System (V)
	MPT (100%)	MPT (90%)	Direct (Optimal)	MPT (90%)	Direct (Optimal)	
10	2.94	2.65	2.83	0.0	0.0	13.8
20	5.41	4.87	5.14	0.2	0.5	14.6
30	6.90	6.21	6.44	4.5	5.6	14.5
40	7.68	6.91	7.11	12.2	14.1	14.4
50	8.16	7.34	7.51	21.3	23.8	14.5
75	8.87	7.98	8.10	48.2	52.2	14.8
100	9.23	8.31	8.40	72.7	82.5	15.2

fall dramatically for a 90-degree tilt, however, to 1.85 million liters. As shown in Figure I-3, graphs of monthly production indicate that the only way to levelize production is to sacrifice production in the summer; even at the best angle for winter production (50 degrees), the ratio of June to December output was 2:1.

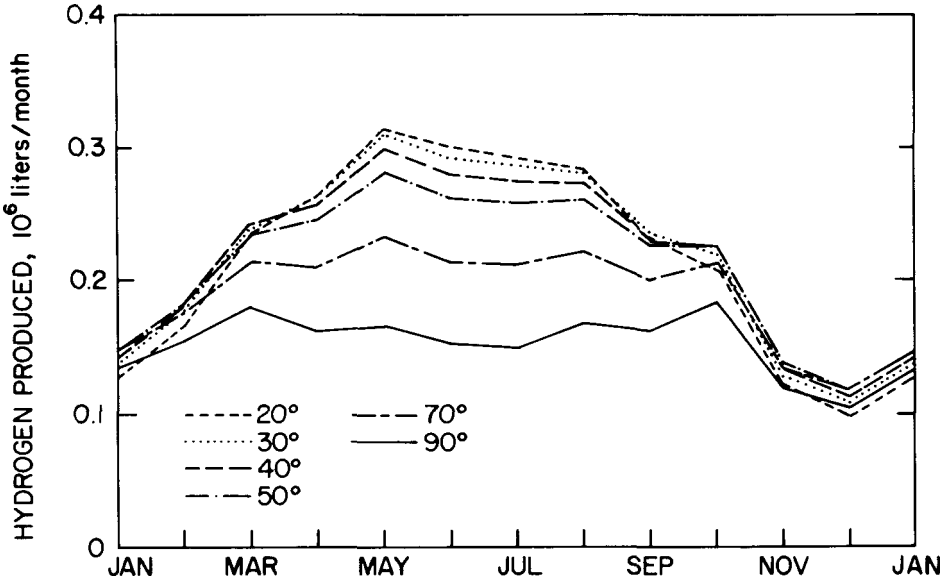

Figure I-3. MPT system monthly hydrogen production for a 10 kW array at various tilt angles.

I-D.4 Directly Coupled System

In the absence of a maximum power tracking system, the wiring configuration of the array can have a major impact on system operation. Wiring more PV cells in series will raise the nominal voltage of the array and and lower the corresponding current; a configuration must be chosen for which the voltage imposed on the PV array by the electrolyzer will result in near optimal operation of the PV array for as much time as possible. Of course, the variety of climatic conditions which occur during a year ensures that any given wiring scheme will be less than optimal a significant fraction of the time; we seek the configuration providing the maximum hydrogen production over the course of a year.

Load matching in PV-electrolyzer systems has previously been addressed by several authors either at a single or small number of operating points, or for a small number of possible voltages (3, 5, 6, 7). Using our simulation model, we have examined these systems over a wide range of PV array voltages and power levels.

The impact of different nominal peak power point voltages is seen clearly in Figure I-4, where annual hydrogen production for several array sizes is shown. The hydrogen production maximizing voltages, which lie in the range of 14 to 15 V for all array sizes, are given in Table I-2 along with the corresponding hydrogen production levels. Figure I-4 makes it clear that the penalties for having too low a voltage are far greater than those resulting from too high a voltage--a prudent planner will ensure that errors result in an array voltage that is slightly above the optimal value, rather than below.

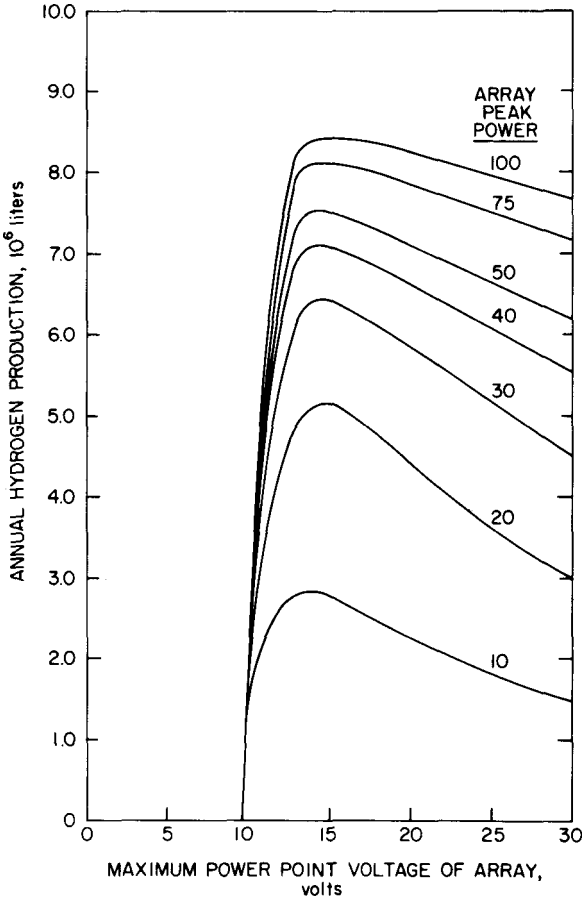

Figure I-4. Annual hydrogen production vs maximum power point voltage of PV array.

The production of excess electricity also depends strongly on the array wiring, as shown in Figure I-5. The maxima here occur at slightly higher voltages, 15 to 16 volts, than do those for hydrogen production. Thus choosing an operating voltage based solely on maximizing hydrogen production may in fact produce a system which is slightly less than optimal economically, if the excess electricity has a high market value.

B199
SPE(A/I)9

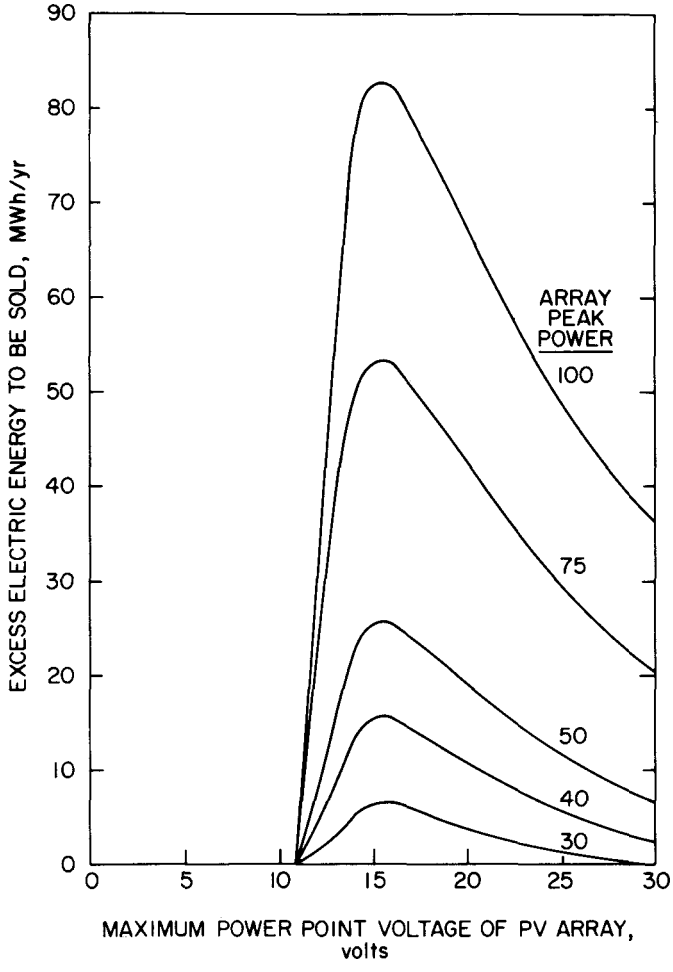

Figure I-5. Annual excess electrical energy vs maximum power point voltage of PV array.

I-D.5 Comparison of MPT vs Directly Coupled Systems

Figure I-2 and Table I-2 compare the annual hydrogen production of the optimal (in terms of annual hydrogen production) directly coupled system (0) to 90% (x) and 100% (+) efficient MPT systems over a wide range of PV array sizes. At all power levels the directly coupled system outperforms the 90% efficient maximum power tracker, in agreement with results reached analytically by Carpetis[5] and Freudenberg[7]. In fact, it is clear from the results in Figure I-2 and Table I-2 that a maximum power tracker must have an efficiency of 93-95% just to break even in energy and be more efficient to break even in excess electricity; it seems unlikely that such a device could possibly pay for itself under any circumstances. In Table I-2, the excess electricity available from the directly coupled system is also shown, and is seen to be substantially in excess of that from the 90% efficient maximum power tracking system.

B199
SPE(A/I)9

I-E. Conclusions

A TRNSYS-based model of a photovoltaic-electrolyzer system has been developed. The program is capable of simulating maximum power tracking or directly coupled system operation. The dependence of annual hydrogen production on PV array size (for fixed electrolyzer capacity) has been determined. Studies of hydrogen production as a function of tilt angle indicate that the seasonal variations in production can only be smoothed by sacrificing summer production.

The simulations show that the optimal array peak power voltage for hydrogen production in the directly coupled mode is close to the nominal electrolyzer voltage. When operating at this voltage, a directly coupled system annually produces about 95% of the hydrogen of a perfectly efficient MPT system. This means that maximum power trackers are probably not desirable in photovoltaic-electrolyzer systems.

At array sizes above 20 kW peak (for a 15 kW electrolyzer) significant maximizes excess electricity production is about 7% above that which maximizes hydrogen production.

B199
SPE(A/I)10.1

REFERENCES

1 Metz, Philip D., "Development of the Brookhaven National Laboratory Integrated Test Bed for Advanced Hydrogen Technology," BNL 32935, presented at the IEA Workshop on Electrolytic Hydrogen Production, Annex IV, Ispra, Italy, May 30-June 1, 1983.

2 Strickland, G. and Schoener, G., "An Integrated Test Bed for Advanced Hydrogen Technology: Photovoltaic/Electrolyzer System," BNL 51577, July 1982.

3 Costogue, E. N. and Yasui, R. K., "Performance Data of a Terrestrial Solar Photovoltaic Water Electrolysis Experiment," 1975 Solar Energy Congress of the International Solar Energy Society, Los Angeles, California.

4 Cox, K. E., "Hydrogen From Solar Energy Via Water Electrolysis," Eleventh Intersociety Energy Conversion Conference Proceedings, State Line, Nevada, 1976, p. 926.

5 Carpetis, C., "A Study of Water Electrolysis with Photovoltaic Energy Conversion," Int. J. Hydrogen Energy, Vol. 7, 1982, p. 287. Also, Carpetis, C., Schnurnberger, W., Seeger, W., and Steeb, H., "Electrolytic Hydrogen by Means of Photovoltaic Conversion," Proc. of the 4th World Hydrogen Energy Conference, Pasadena, California, Vol. 4, p. 1495, 1982.

6 Hancock, O., "Evaluation of a Photovoltaic-Powered Water Electrolyzer: Performance and Economics," Florida Solar Energy Center, Cape Canaveral, Florida, 1983.

7 Freudenberg, K., "Solar Generator Performance With Load Matching to Water Electrolysis," Applied Phys., A 28, 205 (1982).

8 "TRNSYS - A Transient System Simulation Program," Version 10.1, Report 38-10 of the Solar Energy Laboratory, University of Wisconsin, Madison, WI 53706, June 1979.

9 "SOLMET User's Manual" - Volumes 1 and 2, TD-9724, National Oceanic and Atmospheric Administration, National Climatic Center, Asheville, NC, August 1978.

10 Evans, D. L., et al., "TRNSYS - A Transient System Simulation Program," Version 11.1, App. 7, Report 38-11 of the Solar Energy Laboratory, University of Wisconsin, Madison, WI 53706, April 1981, and Evans, D. L., Facinelli, W. A., and Otterbein, R. T., "Combined Photovoltaic/Thermal System Studies," Arizona State University, Dept. of Mechanical Engineering, Tempe, AZ 85281, SAND 78-7031, (1978).

11 Hart, G. W. and Raghuraman, P., "Residential Photovoltaic System Simulation: Thermal Aspects," DOE/ET/20279-183, Proc. of the ASME Solar Energy Division Fourth Annual Technical Conference, Albuquerque, NM, April 1982.

B199
SPE(A/I)11

12 Hart, G. W., "Residential Photovoltaic System Simulation: Electrical Aspects," MIT Lincoln Laboratory, Lexington, MA, DOE/ET/20279-207, June 1982, and Proc. of the Sixteenth IEEE Photovoltaic Specialists Conference, September 1982.

13 Luft, W., Barton, J. R., and Conn, A. A., "Multifaceted Solar Array Performance Determination," TRW Systems Group, Redondo Beach, CA, February 1967.

14 "Solar Cell Array Design Handbook," Vol. 1, 9.2, Jet Propulsion Laboratory, NTIS N77-14193.

15 "Solid Polymer Electrolyte Water Electrolysis Technology Development - Final Report for October 1977-November 1981," General Electric Company, Aerospace Instruments Department, Direct Energy Conversion Programs, Wilmington, MA 01887, DOE/ET/26202-1, p. 108.

16 Ibid, p. 8.

17 Braun, J., University of Wisconsin, private communication.

18 Meinel, A. B. and Meinel, M. P., "Applied Solar Energy - An Introduction," Addison-Wesley, Reading, MA, 1979.

19 Klein, S. A., Beckman, W. A., and Duffie, J. A., "Monthly Average Solar Radiation on Inclined Surfaces for 261 North American Cities," Report 44-2,Solar Energy Laboratory, University of Wisconsin, Madison, WI 53706 (1978).

B199
SPE(A/I)11

APPENDIX II

PHOTOVOLTAIC-ELECTROLYZER SYSTEM ECONOMIC MODEL

II-A Introduction

This appendix describes the economic model which computes the cost of producing hydrogen electrolytically, on which the technoeconomic results presented in Section 3 are based. The economic model is quite simple (e.g., does not consider depreciation, income tax consequences or inflation) so that absolute comparisons between the hydrogen costs generated and real-world market prices should be viewed cautiously. However, the simplicity of the model makes relative comparisons between different operating modes and sensitivity analyses of capital costs, electricity costs, etc. quite transparent.

Three modes of operation have been considered:

- o Grid-Powered Operation
- o Stand-Alone PV-Powered Operation
- o PV Supplemented by 8-Hour/day Off-Peak Grid Electricity

In the grid-powered operating mode, the electrolyzer operates round the clock, 8766 hours/year, subject to an electrolyzer availability factor to account for downtime from maintenance and breakdowns. In the stand-alone PV-powered operating mode, all electricity used to produce hydrogen is derived from the PV array. System performance in this mode is determined from computer transient simulation results described in Appendix I, and validated in Section 2. The third mode, PV supplemented by 8 hour/day off-peak grid electricity, seeks to better utilize the electrolyzer--the stand-alone PV-powered system will operate at most 8-10 hours/day--while also reducing the cost of purchased electricity. Ancillary power requirements are not considered in any mode.

The economic model has been developed into a Basic language computer program on a Commodore 64 microcomputer. Disk copies are available at nominal cost.

II-B. Program Operation

This section describes program inputs, outputs, and computational algorithm.

Program Inputs and Outputs

Table II-1 presents all user-selected program inputs, including input definition and units. Table II-2 presents the program outputs. All outputs are normalized to a nominal 1 kWe capacity electrolyzer.

B199
SPE/A 14

Table II-1
Economic Model Program Inputs

Input Definition	Units
Electrolyzer Installed Capital Cost	($1/kWe)
PV Array Installed Capital Cost	($1/kW peak)
Electricity Cost	(¢/kWh)
Operating and Maintenance (O&M) Cost	(% of Total Capital Cost/year)
Property Taxes	(% of Total Capital Cost/yr)
System Lifetime	Years
Discount Rate	%
Electrolyzer Availability (Fraction of Time System is Available for Use)*	%
Relative Nominal Size PV Array/ Electrolyzer (8 cases are possible)	None
Electrolyzer Capacity Utilization* (Maximum current/maximum current possible)	%
Electrolyzer Efficiency*	%

*Applies to grid-powered operation only

B199
SPE/A 15

Table II-2
Economic Model Program Outputs

Output Definition	Units
Present Value of Annuity Factor $[1-(1+i)^{-n}]/i$ (where i = annual interest rate and n = system lifetime	None
Annual Electricity Sales	kWh/yr
Annual Electricity Purchases	kWh/yr
Annual Hydrogen Production	SCF/yr
Total Net Present Value (NPV) of All Costs	$
Hydrogen Cost	$/SCF

Program Algorithm

The program algorithm consists of three computational sections:

1. Compute the net annual cash outflow of all operating costs and annual hydrogen production.

2. Compute the net present value (NPV) of all capital and operating costs.

3. Compute the annualized cost of hydrogen production.

The algorithms, assumptions, and limitations of each section are now described in detail.

1. Compute net annual cash outflow of all operating costs and annual hydrogen production.

The annual net cash outflow, P, is given by Equation II-1:

$$P = E_{purch} - E_{sales} + E_{O\&M} + E_{ptx} \qquad \text{(II-1)}$$

where

E_{purch} = Annual electricity purchased ($/yr)
E_{sales} = Annual electricity sales ($/yr)
$E_{O\&M}$ = Annual operating and maintenance expense ($/yr)
E_{ptx} = Annual property tax expense ($/yr)

The amount of electricity purchased is computed based on the annual number of hours of grid operation, electricity cost, and electrolyzer availability, capacity utilization, and efficiency.

Annual electricity sales, for PV operation only, are determined from Column 4, Table II-3, given the relative PV array/electrolyzer size. Table II-3 is derived from Table I-2 by renormalizing to a 1 kW electrolyzer, and neglecting dryer losses. Only the optimal directly-coupled case is considered. Table I-2 is based on computer transient simulation results which have been validated by comparison with operational data, as discussed in Sections 2 and 3.

Depreciation and income tax effects are not considered. Electricity prices, O+M expense, and property taxes are assumed constant throughout the system lifetime. Inflation is not considered. Electricity purchases and sales are both made at the same price.

This section also computes annual hydrogen production per nominal kWe electrolyzer capacity. For PV-powered operation, the appropriate figure from Table II-3 is used. For grid operation, annual hydrogen production, H, is given by:

$$H = FC\ E_{purch}/E_{kWh} \qquad \text{(II-2)}$$

where

F = Electrolyzer efficiency
C = Conversion constant (9.9837 SCF/kWh)
E_{purch} = Annual Electricity Sales ($/yr) discussed above
E_{kWh} = Electricity cost ($/kWh)

Table II-3
PV-Electrolyzer System Hydrogen Production
And Annual Electricity Sales

Case	Relative Size PV/SPE (Frac.)	Annual H_2 Production (10^3SCF)	Annual Electricity Sales (kWh)
0	0.	0.	0.
1	0.667	7.329	0.
2	1.333	13.311	33.33
3	2.000	16.678	373.03
4	2.667	18.413	940.00
5	3.333	19.449	1587.00
6	5.000	20.977	3480.00
7	6.667	21.754	5500.00

B199
SPE/A 17

2. Compute the Net Present Value (NPV) of all capital and operating costs.

The net present value of all capital and operating costs, NPV, is given by:

$$NPV = C_E + RC_{pv} + F_a P \qquad \text{(II-3)}$$

where

C_E = Electrolyzer installed capital cost ($/kWe)

R = Relative nominal size PV array/electrolyzer

C_{pv} = PV array installed capital cost ($/kW peak)

F_a = Present value of annuity factor

$$[1 - (1 + i)^{-n}]/i$$

where i = annual interest rate
n = system lifetime

P = annual net cash outflow ($/yr) from Equation (II-1).

Note that no salvage value is allotted to any capital.

3. Compute the annualized cost of hydrogen production.

The annualized cost of hydrogen production ($/SCF), A, is given by:

$$A = \frac{NPV}{HF_a} \qquad \text{(II-4)}$$

where NPV, H, and F_a have all been defined above.

B199
SPE/A 18

APPENDIX III

FITTING EQUATIONS AND COEFFICIENTS

PV Array

Array Power (W/m^2) = Ao + A1(I) + A2$(I)^2$

where I = Insolation in $Watt/m^2$

Mode	Ao (W/m^2)	A1 ( )	A2 $(1/W/m^2)$	Stand. Err.	Stand. Dev.
1*	-3.859	8.984×10^{-2}	-7.829×10^{-6}	1.884×10^{-1}	2.354
2**	-1.691	8.091×10^{-2}	2.748×10^{-6}	9.816×10^{-2}	1.249

Array Voltage (V) = Ao + A1(I) + A2$(I)^2$

where I = Insolation in $Watt/m^2$

Mode	Ao (V)	A1 $V/W/m^2$	A2 $V/(W/m^2)^2$	Stand. Err.	Stand. Dev.
1	28.60	3.218×10^{-3}	-2.731×10^{-6}	1.098×10^{-1}	1.376
2	28.45	3.448×10^{-3}	-1.592×10^{-6}	9.7604×10^{-2}	1.242

DC-DC Converter

DC-DC Power Out [Watt] = Ao + A1(P) + A1$(P)^2$

where P is the DC-DC power in (W)

Mode	Ao (W)	A1 ( )	A2 (1/W)	Stand. Err.	Stand. Dev.
1	-27.43	8.278×10^{-1}	-2.105×10^{-5}	2.695	33.67
2	-18.95	8.369×10^{-1}	-2.599×10^{-5}	2.906	36.99

DC-DC Voltage Out (V) = Ao + A1(P) + A2$(P)^2$

where P is the DC-DC power in (W)

Mode	Ao (V)	A1 (V/W)	A2 (V/W^2)	Stand. Err.	Stand. Dev.
1	11.87	1.213×10^{-3}	-1.160×10^{-7}	1.550×10^{-2}	1.942×10^{-1}
2	13.51	6.731×10^{-4}	-7.670×10^{-8}	4.184×10^{-2}	5.326×10^{-1}

*Mode 1 = 300% boosted PV-powered operation
**Mode 2 = Complementary PV plus grid-powered operation

B199
SPE(A/III)1

SPE Electrolyzer (300% Boosted PV-Powered Mode)

$V/Cell = Ao + A1(I) + A2(I)^2$

where I is the electrolyzer current in Amp

Temp. ±2.5°C	Ao (V)	A1 V/A	A2 V/A^2	Stand. Err.	Stand. Dev.
60	1.452	7.161×10^{-4}	-3.877×10^{-7}	3.745×10^{-3}	1.298×10^{-2}
65	1.465	5.957×10^{-4}	-2.483×10^{-7}	1.930×10^{-3}	1.057×10^{-2}
70	1.464	5.453×10^{-4}	-2.074×10^{-7}	1.220×10^{-3}	7.421×10^{-2}
75	1.468	5.149×10^{-4}	-2.017×10^{-7}	3.615×10^{-3}	2.729×10^{-2}

B199
SPE(A/III)2

☆ U.S. GOVERNMENT PRINTING OFFICE: 1985-611-035/20006